Ligand -mediated Coating of Liposomes with Serum Proteins for Biomedical Applications

佐藤, ひかり

https://doi.org/10.15017/1931748

出版情報：Kyushu University, 2017, 博士（工学）, 課程博士
バージョン：
権利関係：

2018

Doctoral Thesis

Ligand-Mediated Coating of Liposomes with Serum Proteins for Biomedical Applications

Graduate School of Systems Life Sciences

Kyushu University

Hikari Sato

Abstract

Ligand-Mediated Coating of Liposomes with Serum Proteins for Biomedical Applications

Hikari Sato

Doctor of Philosophy
Graduate School of Systems Life Sciences
Kyushu University
2018

This thesis proposes a new strategy for liposome surface modification of serum proteins, which is potentially useful for drug delivery. Liposome surface modification has grown extensively, and improved liposomes for clinical application by enhancing the stability to prolong the blood residence time and specificity to target cell to deliver the drugs. Two major serum proteins, human serum albumin and immunoglobulin G (IgG), show extraordinary long blood circulation time, and have been utilized for exploiting protein-based drug. To introduce the advantage of the proteins into liposomes, serum albumin or IgG-modified liposomes have been developed. Most of liposomes coated with serum proteins have been covalently immobilized, which cannot circumvent the deterioration of the proteins' characteristics and takes time for production. In contrast, ligand-mediated coating of surface is stable and has been expected to modulate the denaturation of the proteins. Furthermore, abundant endogenous proteins can be utilized for *in situ* coating after administration. In the present thesis, I developed a ligand-mediated coating method for the preparation of

serum albumin or IgG-coated liposomes.

In Chapter 2 and 3, serum albumin-coated liposomes were exploited. Among numerous ligands of serum albumin, two types of ligands were selected. The first one was bilirubin, which is known to have the highest binding affinity among the reported ligands. The coating of liposomes with serum albumin and the reversibility of the coating were successfully monitored. However, it was found that the serum albumin-binding ratio to bilirubin on liposome surface was lower than that expected. This relatively low binding ratio may result from the hydrophobic nature of bilirubin. Then, the second one was alkyl chains. I used three types of alkyl chains with different chain length with or without terminal negative charge, and achieved coating of liposome surfaces with serum albumin via the ligands. A relatively short alkyl ligand or a long alkyl ligand with terminal carboxylate could be exposed on the liposome surface without causing aggregation of the liposomes and these ligands could subsequently bind HSA to significantly improve the colloidal stability of the liposomes. The resulting HSA-coated liposomes were as inert as conventional PEGylated liposomes in terms of macrophage recognition. This HSA coating has a possibility to improve the stability of the liposomes in blood for drug delivery system.

In Chapter 4, I proposed IgG-coating of liposomes by using Fc-binding peptide. Fc-III peptide was used as a Fc-binding ligand. To modify the peptide onto the liposome surface, Fc-III peptide was palmitoylated on its N-terminus. The liposomes containing palmitoylated Fc-III were successfully coated with IgG. I examined the recognition of IgG coated on the liposomes toward cell surface receptors. The anti-CD20-coated liposomes bound to a human B lymphoid cell line overexpressing CD20. In contrast, the IgG-coated liposomes were not recognized by macrophages expressing FcγRs, which bind to Fc regions. This strategy may enable coating of liposomes with endogenous IgG in blood after injection and provide stealth

characteristics to the liposomes.

The ligand-mediated coating of liposomes proposed here will extend the current liposome technology. I believe that this strategy has a potential to clinical applications because it enables *in situ* coating.

Table of contents

CHAPTER 1

General Introduction

1.1. Liposomes used as drug carrier

Since Alec Bangham et al. first described the artificial lipid vesicles in 1961 [1], liposome has been extensively researched and developed as high-performance vehicles in the field of drug delivery because of their biocompatibility, biodegradability, and ability to encapsulate both hydrophilic drugs (in the inner core) and hydrophobic drugs (in the bilayer). In addition to the fundamental characteristics, by exploits of liposomal surface modification and tunable membrane characteristics, the liposome technology has grown drastically, and improved liposome for cancer therapy, vaccine, and fungal diseases. At the present time, more than a dozen liposome-based drugs has been approved by Food and Drug Administration (FDA) for clinical use and a number of liposomes are in clinical trials, most of which are available for intravenous applications (**Table 1.1**) [2,3]. As shown in **Table 1.1**, liposomes for drug delivery are composed of at least two phospholipids, of which alkyl chain length, unsaturation of the chain, head group structure, and functional group on head group influence the characteristics and performance of liposome [2,4].

Nowadays, variety of surface modification methods have been proposed to improve the blood half-life of liposomes, the accumulation efficacy to deliver the desired drugs and the targeting efficacy to deliver to desired site. These strategies include the modification of hydrophilic polymers (e.g. polyethylene glycol (PEG)), antibodies (immunoliposomes), and peptides, and some of these liposomes have been in pre-clinical and clinical trials [5-7]. In addition to the direct covalent modification of

functional group on lipid, ligand modification and organizing lipid charge enables modification of functional group on liposome surface [8,9]. Especially, specific non-covalent ligand-mediated modification enables control of binding orientation and stable immobilization [10]. Novel liposomal surface modification technology will enable further growth of drug delivery system.

Table 1.1. FDA-approved liposome-based drugs on the market [2].

Product	Administration	Drug	Particle type	Lipid composition	Indication
Ambisome	Intravenous	Amphotericin B	Liposome	HSPC, DSPG, cholesterol and amphoteracin B in 2:0.8:1:0.4 molar ratio	Sever fungal infections
Abelcet	Intravenous	Amphotericin B	Lipid complex	DMPC and DMPG in 7:3 molar ratio	Sever fungal infections
Amphotec	Intravenous	Amphotericin B	Lipid complex	Cholesteryl sulfate	Sever fungal infections
DaunoXome	Intravenous	Daunorubicin	Liposome	DSPC and cholesterol (2:1 molar ratio)	Blood tumors
DepoCyt	Spinal	Cytarabine	Liposome	DOPC, DPPG, cholesterol and triolein	Neoplastic meningitis and lymphomatous meningitis
DepoDur	Epidural	Morphone sulfate	Liposome	DOPC, DPPG, cholesterol and triolein	Pain
Doxil	Intravenous	Doxorubicin	PEGylated liposome	HSPC:cholesterol:PEG 2000-DSPE (56:39:5 molar ratio)	Kaposi's sarcoma, Ovarian/ Breast Cancer
Epaxal	Intramuscular	Inactivated hepatitis A virus (strain RGSB)	Liposome	DOPC:DOPE (75:25 molar ratio)	Hepatitis A
Inflexal	Intramuscular	Inactivated hemaglutinine of Influenza virus strains A and B	Liposome	DOPC:DOPE (75:25 molar ratio)	Influenza
Lipodox	Intravenous	Doxorubicin	PEGylated liposome	HSPC:cholesterol:PEG 2000-DSPE (56:39:5 molar ratio)	Kaposi's sarcoma, Ovarian/ Breast Cancer
Myocet	Intravenous	Doxorubicin	Liposome	EPC:cholesterol (55:45 molar ratio)	Combination therapy with cyclophosphamide in metastatic breast cancer
Marqibo	Intravenous	Vincristine	Liposome	Sphingomyelin, cholesterol	Acute lymphoblastic leukemia
Visudyne	Intravenous	Verteporphin	Liposome	EPG and DMPC	Macular degeneration

1.2. Two major serum proteins; serum albumin and immunoglobulin G

Serum albumin and immunoglobulin G (IgG) are the most abundant plasma proteins in the bloodstream, representing over 80-90% of the total protein pool [11]. Serum albumin is a heart-shaped protein, which is synthesized by hepatocyte in the liver (~150 mg/kg/day) and works as a carrier of hydrophobic endogenous and exogeneous ligands such as fatty acids, hormones, amino acids as well as drugs [12,13]. IgG is a Y-shaped protein, which is synthesized by plasma cells in the bone marrow (~33 mg/kg/day), lymph nodes and spleen in immune response to foreign substances (antigens) and works as a mediator of immune system to protect body from infections [11,14,15]. Although the structure and functions are totally different, both serum albumin and IgG show the longest blood half-life (~20 days in human) among plasma proteins. This extraordinarily long residence time is attributed to the presence of neonatal Fc receptor (FcRn), which is widely distributed in both vascular endothelial cells, epithelial cells (e.g. placental, epidermal, intestinal, and renal glomerular) from various organs, as well as hematopoietic cells (e.g. B cells, macrophages, and dendritic cells) [11,16-18]. FcRn is a heterodimeric receptor, which binds to serum albumin and IgG at independent binding sites (**Figure 1.1**), and prevents the degradation in intracellular catabolism via pH-dependent recycling and transcytosis pathways (**Figure 1.2**) [19]. As shown in **Figure 1.2**, at endothelial cells, serum albumin and IgG are internalized by cells through non-specific pinocytosis, and follows the endosomal pathway, in which pH decreases to 6, resulting in the association with endosomal FcRn. The protein-FcRn complex is returned to the cell surface, where the proteins are subsequently released into neutral pH blood circulation due to the decrease of affinity to FcRn. On the other hand, at epithelial cells presenting acidic pH, FcRn-mediated

transcytosis takes place. The transcytosis follows a similar pathway, although the proteins directly associate with FcRn on cell surface and are released into the interstitial tissue space. To utilize these recycling/transcytosis mechanism in drug delivery for enhancement of the therapeutic efficacy, not only FcRn-binding domain of serum albumin/IgG but also serum albumin/IgG moelecule-based drugs have been developed [19].

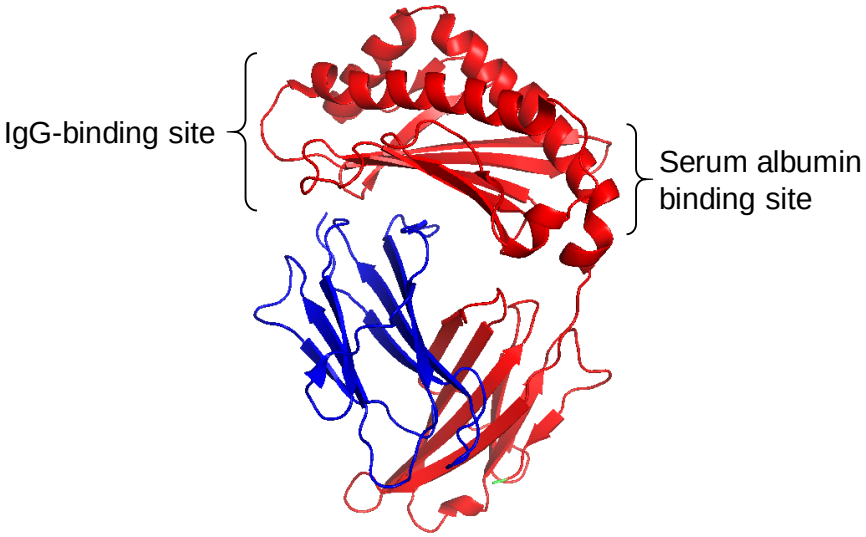

Figure 1.1. Crystal structure of extracellular domain of FcRn and its IgG- and albumin-binding sites (PDB ID: 4N0F).

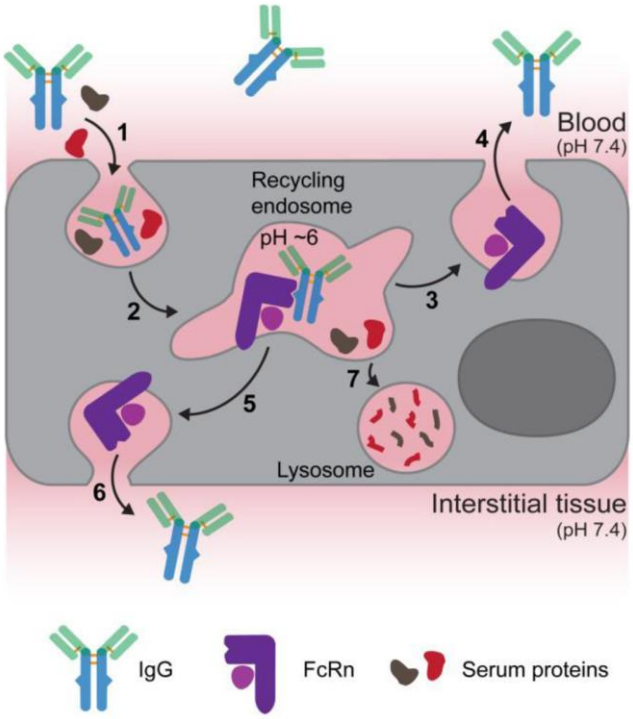

Figure 1.2. FcRn-mediated IgG recycling [19]. At pH 6, FcRn binds to IgG more stably, while at neutral pH, the complex is dissociated. © 2015 Elsevier B.V.

1.2.1. Application of Serum albumin for drug delivery

Serum albumin is the most abundant and water-soluble plasma protein (~40 mg/L in human serum), and works as a carrier protein in blood due to the flexible structure which enables binding to a great number of endogenous and exogenous small molecules [11]. The three-dimensional structure of serum albumin and the complex with ligands have been elucidated by X-ray analysis. As shown in **Figure 1.3**, HSA has relatively small size (8 × 8 × 3 nm) and is composed of three domains (I to III) and each one is divided into two subdomains (A, B). HSA provides a variety of sites to numerous ligand, such as endogenous ligands (e.g., fatty acids, hormones, and hemin), metal ions (e.g., calcium, zinc, and coper) and exogenous drug (e.g., paclitaxel, warfarin, and ibuprofen) [20-22]. Domain I and III interacts with FcRn, and it enhances the blood residence of serum albumin. Furthermore, serum albumin is not

immunogenic.

To provide biocompatibility to materials, serum albumin has been used to coat the surface by covalent or non-covalent (e.g. electrostatic or hydrophobic interaction) [23-34]. Bovine serum albumin as well as human serum albumin have been used for the surface modification of biomaterials due to the high sequence homology (76%) of these two serum albumins. The albumin coating prevents plasma protein and platelet adhesion and suppress thrombogenicity, resulting in improvement of the biocompatibility of materials, and the coating also plays a role to prevent bacterial adherence [23-27]. In the covalent coating, serum albumin forms stable layer on the surface [23-27], while the immobilized serum albumin cannot be replaced with fresh one. As for nonspecific non-covalent coating using physical adsorption via electrostatic or hydrophobic interaction, adsorbed serum albumin can be replaced with fresh one [28-30], although in some materials and pH, it can cause structural change of the serum albumin [29,30]. On the other hand, non-covalent coating via specific ligand is not only reversible but also high affinity interaction, and is expected to overcome the drawback of both covalent and nonspecific non-covalent coating. Serum albumin has three strong binding pockets and four weak binding pockets to relatively long alkyl chains, of which high affinity show K_d ~10^{-9} M [35,36]. The specific association with stearic acid (C18) or palmitic acid (C16) has been adopted for the surface coating of polyurethane-based implants [31-33] and catheters [34]. These can assemble endogenous serum albumin on the surface, of which biocompatibility is expected to be further improved.

Drug delivery system utilizes serum albumin as a carrier, in which genetic fusion with peptides, covalent or non-covalent association has been employed (**Figure 1.4**) [37]. The number of albumin-based drugs are in clinical trials and some of them have already been marketed, which represents growth of interest in the pharmaceutical

application of serum albumin (**Table 1.2**) [20]. The most advanced albumin-based nanoparticle technology is nab-technology, which is a conjugate formation under high pressure to form the particle of human serum albumin and hydrophobic drugs [37]. This technology improves maximum dose of hydrophobic drugs by enhancing the solubility of the drugs in blood. Abraxane is the first approved nab-technology-based product by FDA, and it has the ability not only to be dissolved in blood also to accumulate in the tumor. 60-kDa glycoprotein (gp60)-mediated transport pathway enhances the accumulation to tumor-surrounding interstitium as well as enhanced and permeation effect depending on the particle size [37]. Gp60 expressing on endothelial cell is an albumin receptor, which is responsible for albumin transcytosis [38,39]. The Abraxane in interstitium is believed to be subsequently accumulated to tumor by secreted protein, acidic and rich in cysteine (SPARC), which is overexpressed on tumor cells and bind to albumin [40]. On the other hand, the ability of albumin to bind to alkyl chain has been applied specifically to the development of insulin analogs, e.g. Levemir (insulin detemir) and Tresiba (Insulin degludec) by Novo Nordisk, for the treatment of diabetes [40,41]. The former is a drug, in which a fatty acid (myristic acid, C14) is bound to the lysine residue (**Figure 1.5**) [37]. After Levemir is subcutaneously injected as a hexameric assembly, which is too large to pass through capillary fenestrate, the interstitial albumin subsequently binds to Levemir in the depot, followed by binding to plasma albumin through its fatty acid. The length of the fatty acid modified on insulin affects the binding affinity to HSA resulting in the difference in half-life and bioavailability [42]. The terminal half-life of Levemir is extended from 4 to 6 min for native insulin to 5 to 7 h [43]. Tresiba is an insulin derivative modified with hexadecandioic acid, and its affinity to human serum albumin is reported to be 2.4-folds higher than Levemir, and the terminal half-life is 17-25 h, which is 3- to 4-folds higher than Levemir [41,44]. This high affinity to serum albumin is probably

because the pockets of serum albumin have cationic amino acids at the bottom to bind with anionic carboxylates on the terminus of fatty acids [45]. The tunable affinity by selection of ligands enables to control pharmacokinetics of drugs.

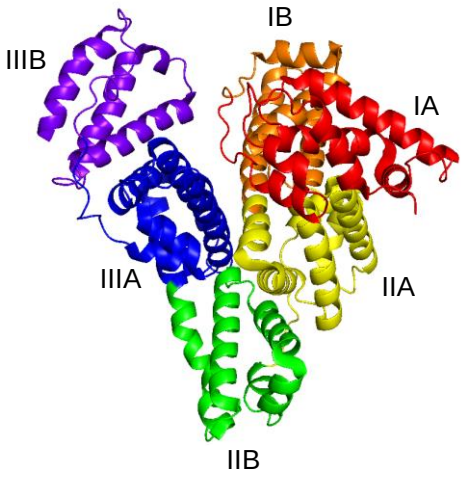

Figure 1.3. Crystal structure of human serum albumin. The three domains composed each two subdomains are colored in red (IA), orange (IB), yellow (IIA), green (IIB), blue (IIIA), and purple (IIIB). The figure was designed using PyMOL (DeLano Scientific) using data from PDB ID: 4K2C.

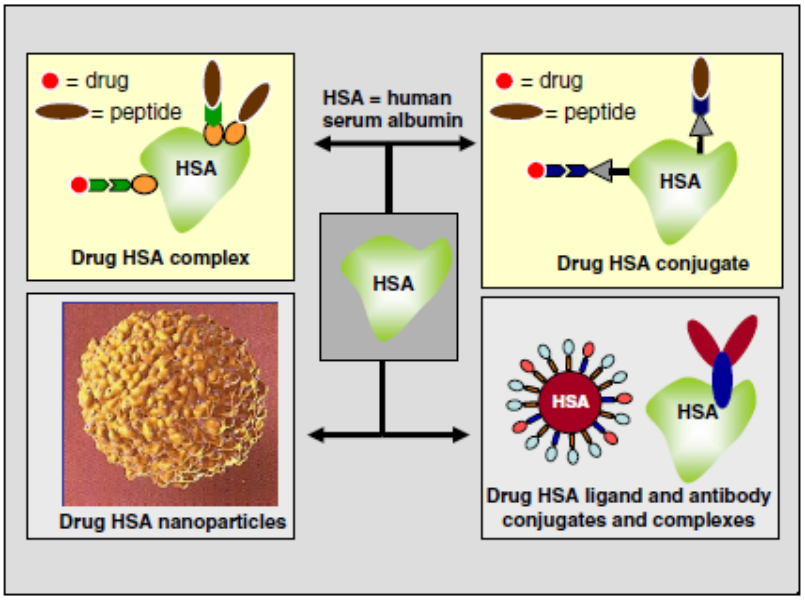

Figure 1.4. Serum albumin-based drugs for developing drug-, peptide- or Abs-based drugs as conjugates, complexes or nanoparticles [37]. © 2011 Elsevier B.V.

Table 1.2. A selection of albumin-based drugs in clinical trials and marketed products [20]. © 2016 Larsen et al.

Attachment	Name	Disease	Drug type	Clinical status	Company
Non-covalent/reversible association	Levemir®	Diabetes type 1 and 2	Insulin detemir	Marketed	Novo Nordisk
	Victoza®	Diabetes type 2	GLP-1	Marketed	Novo Nordisk
	Ozoralizumab	Rheumatoid arthritis	Antibody derivative	Phase II completed	Ablynx
Covalent	MTX-HSA	Cancer and autoimmune diseases	Methotrexate	Phase II	Access Pharmaceuticals Inc.
	Aldoxorubicin	Cancer	Doxorubicin	Phase I completed	CytRx, Inc.
	CJC-1134	Diabetes type 2	Exendin-4	Phase II	ConjuChem
Genetic fusion	Eperzan/Tanzeum	Diabetes type 2	GLP-1	Marketed	Glaxo Smith Kline
	N/A	Hemophilia	FVIIa	Phase I completed	CSL Behring GmbH
	N/A	Hemophilia B	rIX-FP	Phase III completed	CSL Behring GmbH
	Albuferon®/Zalbin/Jouleferon	Hepatitis C	INFalpha-2b	Phase III completed, Development ceased	Human Genome Sciences in collaboration with Novartis
Micro-/Nanoparticle	Abraxane®	Cancer	Paclitaxel	Marketed	Celgene
	ABI-008	Cancer	Docetaxel	Phase I/II	Celgene
	ABI-009	Cancer	Rapamycin	Phase I/II	Celgene
	ABI-010	Cancer	HSP90 Inhibitor	Withdrawn before enrollment	Celgene
	^{99m}Tc-Albures	Diagnostic purpose	Technetium-99	Marketed	GE Healthcare
	^{99m}Tc-Nanocoll	Diagnostic purpose	Technetium-99	Marketed	GE Healthcare

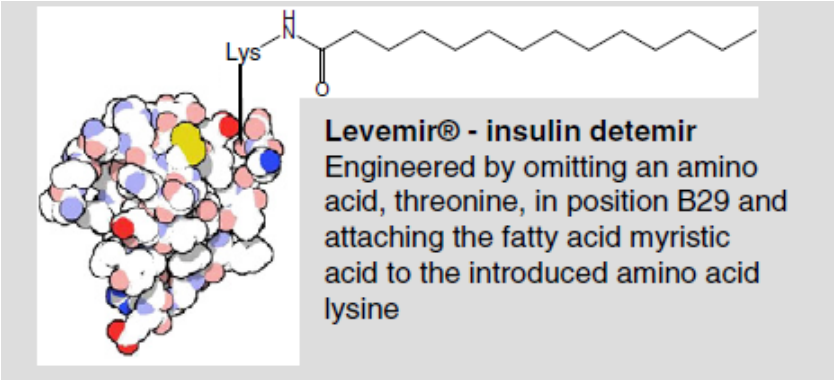

Figure 1.5. Structure of Levemir [37]. © 2011 Elsevier B. V.

1.2.2. Serum albumin-coated liposome

Surface coating with serum albumin has been adopted to nanoparticles including liposomes to prevent clearance in a short time and prolong the blood circulation time by improving the colloidal stability in blood, suppressing the recognition by antibodies and complements on the surface as well as enhancing the uptake from tumor via gp60 and SPARC [20,46]. Covalent and nonspecific non-covalent coating of liposomes have been reported [47-50], while non-covalent coating of nanoparticles via specific ligand is less common, and such liposome has not been reported. This is because the albumin-binding ligands have high hydrophobicity and tend to bury into hydrophobic liposome bilayer rather than exposed to the aqueous phase [51].

1.2.3. Application of immunoglobulin G (IgG) for drug delivery

Immunoglobulin G (IgG) is the second most abundant plasma protein (~11 mg/ml in human serum) and the most abundant antibody (Ab), and works as mediators of immune response causing cytotoxicity. The Y-shaped structure (>150 kDa) of IgG is divided into two domains, fragment antigen-binding (Fab) regions and a fragment crystallizable (Fc) regions (**Figure 1.6**). Fab regions have variable regions showing

different sequence between IgGs, and bind to antigens with high affinity and specificity. On the other hand, Fc regions show identical sequence between IgGs and bind to Fc receptor expressed on effector cells and complements, which trigger activation of immune responses [11,14,15]. The Fc region binds also to FcRn depending on pH, and it enhances the blood residence of IgG [16].

The high specificity to antigen, immune activation, and long blood retention of IgG are leading to the development of high selective and long acting therapeutic drugs. Not only therapeutic monoclonal antibodies but also mAb-based technology including Fc-fusion proteins, antibody fragments, antibody-drug conjugates (ADCs), immunotoxins, and immunoliposomes have been developed [6].

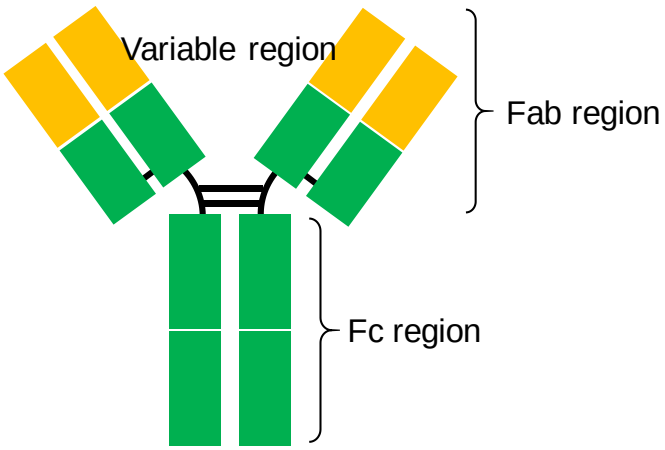

Figure 1.6. Structure of IgG antibody. Yellow regions show variable regions, and green regions show constant regions.

1.2.4. IgG-coated liposome

Surface coating with IgG or their fragment has been adopted for polymeric nanoparticles, inorganic particles, and liposomes to target the specific site bound with Fab region and to subsequently induce immune response toward target cells by effector cells bound with Fc region. The multiple modification of IgG on the nanoparticle surface enhances targeting ability to antigens due to the increased valency. Besides the targeting ability and the induced cytotoxicity effect, the combination of IgG and nanoparticle encapsulating drugs enables to deliver larger amount of drug into targeted cells than IgG molecule itself [6]. As for IgG-coated liposome, the conjugation is known as immunoliposomes, some of which are under clinical trials (**Table 1.3**) [6].

In general, coating nanoparticles surface with IgG is carried out through covalent bonding, nonspecific non-covalent interaction via physical adsorption (e.g. electrostatic and hydrophobic interaction) [52], or specific non-covalent interaction via adapter molecules (e.g. streptavidin-biotin interaction and protein A-Fc region) [53-55]. Coating nanoparticle surface using covalent bonding, nonspecific non-covalent interaction, and streptavidin-biotin interaction enables stable immobilization of IgG on surface, while such technique causes random orientation of antibody [10]. In contrast, coating surface using specific non-covalent interaction is advantageous because it enables stable modification via specific binding site without losing antibody activity.

Table 1.3. Immunoliposomal drugs in pre-clinical and clinical development [6]. © 2013 Elsevier Inc.

Antibody	Target	Payload	Stage	Indication
Anti-CD19	CD19	Doxorubicin, vincristine	Pre-clinical	B-cell lymphoma Multiple myeloma
Anti-Her2 (F5-scFv)	HER2	Doxorubicin	Clinical (Phase I)	Breast cancer
Anti-Her2-Fab′ (scFv C6.5)	HER2	Doxorubicin	Pre-clinical	Breast cancer
Anti-CEA 21B2	Carcinoembryonic antigen, CEA	Doxorubicin	Pre-clinical	Gastric cancer
Anti-β_1-integrin Fab′	β_1 integrins	Doxorubicin	Pre-clinical	Non-small cell lung carcinoma
Anti-GD_2, anti-GD_2 Fab′	GD_2	Doxorubicin	Pre-clinical	Neuroblastoma, melanoma
Anti-EGFR C225 Fab′	EGFR	Doxorubicin	Clinical (Phase I completed)	Solid tumors

1.3. Overview of this thesis

Various surface modifications of liposome have been developed for exploiting wide application of therapeutic use. Surface coating of liposomes with serum albumin is useful because serum albumin-coating avoids recognition by antibodies and complements as well as improves colloidal stability to extend blood circulation time. IgG-coating of liposome can mediate the uptake by cells expressing target receptors (as immunoliposome) and enhancing healing. Covalently modified serum albumin and IgG do not allow exchange reaction with fresh one, which is not able to resist to the deterioration in the characteristics. On the other hand, coating of surface with specific interaction between ligand and the proteins is strong and has been expected to avoid the denaturation of the proteins and protect the target binding site. Furthermore, the modification procedure is simple and no need of protein modification. In the present thesis, I propose serum albumin and IgG-coated liposomes via specific ligands.

To coat the surface of liposome with serum albumin, covalent bond or nonspecific physical interaction have been exploited so far [47-50], and the surface coating of liposome via the specific interaction between the hydrophobic pockets of serum albumin have not been reported. This is because of difficulty to expose the hydrophobic ligands into aqueous phase on the surface of liposomes prior to binding with serum albumin. In liposomes, the hydrophobic ligands tend to be buried into liposomal membrane rather than exposed to aqueous phase. Thus, I developed two types of ligand-modified liposome. In Chapter 2, bilirubin, which is known as endogenous ligand to serum albumin and has high affinity to serum albumin, was adopted as a ligand. Bilirubin has negative charge, which will prevent burying in hydrophobic membrane. The bilirubin was bound to the terminus of PEG-modified

phospholipid, and the liposome was prepared by a hydration method. The reversible coating on liposome was examined by using fluorophore-modified albumin. In Chapter 3, three types of alkyl chains with different chain length with or without terminus charge were used as ligands. It was found that a relatively short alkyl ligand or a long alkyl ligand with terminal carboxylate could be exposed on the liposome surface without causing aggregation of the liposomes and these ligands could subsequently bind albumin to significantly improve the colloidal stability of the liposomes. The resulting albumin-coated liposomes were as inert as conventional PEGylated liposomes in terms of macrophage recognition.

In Chapter 4, to coat liposome with IgG, I developed IgG-binding peptide-modified liposome. Some liposomes containing Ab-binding molecule have been reported so far [6]. Here Fc region binding peptide (Fc-III) was focused on as a ligand, which can bind to abundant endogenous IgG with strong binding affinity (K_d = 25 nM). To load the peptide into liposome surface, palmitoylated Fc-III was synthesized by Fmoc solid phase peptide synthesis, and the liposome was prepared by a hydration method. The stable coating of liposome by fluorophore-modified IgG was successfully monitored by fluorescence correlation spectrometry. The liposome showed the stable dispersion dependent on the IgG concentration. The recognition of the IgG coated on liposome by a cell expressing antigen protein was observed, while the uptake of the liposome by macrophage expressing FcγRs was not observed. Thus, the liposome coated with IgG is expected to show stealth characteristics in blood.

Chapter 5 summarizes the findings and discussions described in this thesis. Then, the perspectives of this research are described.

1.4. References

[1] Bangham, A.D.; Standish, M. M.; Watkins, J. C. Diffusion of univalentions across the lamellae of swollen phospholipids. *J. Mol. Biol*. **1965**, 13, 238-252.

[2] Zylberberg, C.; Matosevic, S. Pharmaceutical liposomal drug delivery: a review of new delivery systems and a look at the regulatory landscape. *Drug Deliv.* **2016**, 23, 3319-3329.

[3] Bozzuto, G.; Molinari, A. Liposomes as nanomedical devices. Int. *J. Nanomed.* **2015**, *10*, 975-999.

[4] Bulbake, U.; Doppalapudi, S.; Kommineni, N.; Khan, W. Liposomal formulations in clinical use: an updated review. *Pharmaceutics* **2017**, *9*, 12.

[5] Sercombe, L.; Veerati, T.; Moheimani, F.; Wu, S. Y.; Sood, A. K.; Hua, S. Advances and challenges of liposome assisted drug delivery. *Front Pharmaco.* **2015**, *6*, 286

[6] Sapra, P.; Shor, B. Monoclonal antibody-based therapies in cancer: advances and challenges. *Pharmacol. Ther.* **2013**, *138*, 452-496.

[7] Hagimori, M.; Fuchigami, Y.; Kawakami, S. Peptide-based cancer-targeted DDS and molecular imaging. *Chem. Pharm. Bull.* **2017**, 65, 618-624.

[8] Loughrey, H.; Bally, M. B.; Cullis, P. R. A non-covalent method of attaching antibodies to liposomes. *Biochim. Biophys. Acta* **1987**, *901*, 157-160.

[9] Balazs, D. A.; Godbey, W. Liposomes for use in gene delivery. J. Drug Deliv. **2011**, *2011*, 326497.

[10] Arruebo, M.; Valladares, M.; González-Fernández Á. Antibody-conjugated nanoparticles for biomedical applications. *J. Nanomater.* **2009**, *2009*, 439389.

[11] Sand, K. M. K.; Bern, M.; Nilsen, J.; Noordzij, H. T.; Sandlie, I.; Andersen, J. T. Unraveling the interaction between FcRn and albumin: opportunities for design of

albumin-based therapeutics. *Front Immunol.* **2015**, *5*, 682

[12] Levitt, D. G.; Levitt, M. D. Human serum albumin homeostasis: a new look at the roles of synthesis catabolism, renal and gastrointestinal excretion, and the clinical value of serum albumin measurements. *Int. J. Gen. Med.* **2016**, *9*, 229-255.

[13] Peters, T. Jr. All about Albumin: Biochemistry, Genetics and Medical Applications; Academic Press, Inc.: Orlando, FL, 1996

[14] Van Furth, R. The formation of immunoglobulins by human tissues in vitro III. spleen, lymph nodes, bone marrow and thymus. *Immunology* **1966**, *11*, 13-18.

[15] Ferenčík, M. Handbook of Immunochemistry, Springer: Dordrecht, Holland, 1993

[16] Sleep, D.; Cameron, J.; Evans, L. R. Albumin as a versatile platform for drug half-life extension. *Biochim. Biophys. Acta* **2013**, *1830*, 5526-5534.

[17] Cianga, C.; Cianga, P.; Plamadeala, P.; Amalinei, C. Nonclassical major histocompatibility complex (I-like Fc neonatal receptor (FcRn) expression in neonatal human tissues. Hum. Immunol. **2011**, *72*, 1176-1187.

[18] Baker, K.; Rath, T.; Michal, P.; Blumberg, R. S. The role of FcRn in antigen presentation. Front Immunol. 2014, 5, 408.

[19] Sockolosky J. T.; Szoka, F. C. The neonatal Fc receptor, FcRn, as a target for drug delivery and therapy. *Adv. Drug Deliv. Rev.* **2015**, 91, 109-124.

[20] Larsen, M. T.; Kuhlmann, M.; Hvam, M. L.; Howard, K. A. Albumin-based drug delivery: harnessing nature to cure disease. Mol. Cell. Ther. **2016**, 4:3.

[21] Prinsen, B. H. C. M. T.; de Sain-van der Velden, M. G. M. Albumin turnover: experimental approach and its application in health and renal diseases. *Clin. Chim. Acta* **2004**, *347*, 1-14

[22] Sugio, S.; Kashima, A.; Mochizuki, S.; Noda, M.; Kobayashi, K. Crystal structure of human serum albumin at 2.5 Å resolution, *Protien Eng.* **1999**, *12*, 439-446

[23] Addonizio, V. P. Jr; Macarak, J.; Nicolaou, K. C.; Edmunds, L H. Jr; Colman, R. W.

Effects of prostacyclin and albumin on platelet loss during in vitro simulation of extracorporeal circulation. *Blood* **1973**, *53*, 1033-1042

[24] Kottke-Marchant, Kandice; Anderson, J. M.; Umemura, Y.; Marchant, R. E. Effect of albumin coating on the in vitro blood compatibility of Dacron® arterial prostheses. Biomaterials **1989**, *10*, 147-155

[25] An, Y. H.; Stuart, G. W.; McDowell, S. J.; McDaniel, S. E.; Kang, Q.; Friedman, R. J. Prevention of bacterial adherence to implant surfaces with a cross linked albumin coating in vitro, J. Orthop. Res. **1996**, *14*, 846-849

[26] Steffens, G. C. M.; Nothdurft, L.; Buse, G.; Thissen, H.; Hocker, H.; Klee, D. High density binding of proteins and peptides to poly(D,L-lactide) grafted with polyacrylic acid. *Biomaterials* **2002**, *23*, 3523-3531.

[27] Ulbricht, M.; Riedel, M. Ultrafiltration membrane surfaces with grafted polymer 'tentacles': preparation, characterization and application for covalent protein binding. *Biomaterials* **1998**, *19*, 1229-1237.

[28] Jeyachandran, Y. L.; Mielczarski, E.; Rai, B.; Mielczarski, J. A. Quantitative and qualitative evaluation of adsorption/desorption of bovine serum albumin on hydrophilic and hydrophobic surfaces. *Langmuir* **2009**, *19*, 11614-11620.

[29] Vermonden, T.; Giacomelli, C. E.; Norde, W. Reversibility of structural rearrangements in bovine serum albumin during homomolecular exchange from AgI particles. *Langmuir* **2001**, *17*, 3734-3740.

[30] Norde, W.; Giacomelli, C. E. BSA structural changes during homomolecular exchange between the adsorbed and the dissolved states. *J. Biotechnol.* **2000**, *79*, 259-268.

[31] Eberhart, R. C.; Munro, M. S.; Williams, G. B.; Kulkarni, P. V.; Shannon, W. A. Jr.; Brink, B. E.; Fry, W. J. Albumin adsorption and retention on

C_{18}-alkyl-derivatized polyurethane vascular grafts. *Artif. Organs.* **1987**, *11*, 375-382.

[32] Pitt, W. G.; Cooper, S. L. Albumin adsorption on alkyl chain derivatized polyurethanes: I. the effect of C-18 alkylation. *J. Biomed. Mater. Res.* **1988**, *22*, 359-382.

[33] Pitt, W. G.; Grasel, T. G.; Cooper, S. L. Albumin adsorption on alkyl chain derivatized polyurethanes. II. The effect of alkyl chain length. *Biomaterials* **1988**, *9*, 36-46.

[34] Wang, D.; Ji, J.; Gao, C.; Yu, G.; Feng, L. Surface coating of stearyl poly(ethylene oxide) coupling-polymer on polyurethane guiding catheters with poly(ether urethane) film-building additive for biomedical applications. *Biomaterials* **2001**, *22*, 1549-1562.

[35] Simard, J. R.; Zunszain, P. A. Hamilton, J. A.; Curry, S. Location of high and low affinity fatty acid binding sites on human serum albumin revealed by NMR drug-competition analysis, *J. Mol. Biol.* **2006**, *361*, 336-351

[36] Richieri, G. V.; Anel, A.; Kleinfeld, A. M. Interactions of long-chain fatty acids and albumin: determination of free fatty acid levels using the fluorescent probe ADIFAB. *Biochemistry* **1993**, *32*, 7574-7580.

[37] Elsadek, B.; Kratz, F. Impact of albumin on drug delivery – new applications on the horizon. *J. Control. Release* **2012**, 157, 4-28.

[38] Tiruppathi, C.; Song, W.; Bergenfeldt, M.; Sass, P.; Malik, A. B. Gp60 activation mediates albumin transcytosis in endothelial cells by tyrosine kinase-dependent pathway. *J. Biol. Chem.* **1997**, *272*, 25968-25975.

[39] Wang, Z.; Tiruppathi, C.; Minshall, R. D.; Malik, A. B. Size and dynamics of caveolae studied using nanoparticles in living endothelial cells, *ACS nano*, **2009**, *3*, 4110-4119.

[40] Hawkins, M. J.; Soon-Shiong, P.; Desai, N. Protein nanoparticles as drug carriers in clinical medicine. *Adv. Drug Deliv. Rev.* **2008**, *60*, 876-885.

[41] Jonassen, I.; Havelund, S.; Hoeg-Jensen, T.; Steensgaard, D. B.; Wahlund, P. O.; Ribel, U. Design of the novel protraction mechanism of insulin degludec, an ultra-long-acting basal insulin. *Pharm. Res.* **2012**, 39, 2104-2114.

[42] Havelund, S.; Plum, A.; Ribel, U.; Jonassen, I.; Vølund, A.; Markussen, J.; Kurtzhals, P. The mechanism of protraction of insulin detemir, a long-acting, acylated analog of human insulin. *Pharm, Res.* **2004**, 21, 1498-1504.

[43] Danne, T.; Lüpke, K.; Walte, K.; Von Schuetz, W.; Gall, M. A.; Insulin detemir is characterized by a consistent pharmacokinetic profile across age-groups in children, adolescents, and adults with type 1 diabates. *Diabetes Care*, **2003**, 26, 3087-3092.

[44] Tambascia, M. A.; Eliaschewitz, F. G. Degludec: the new ultra-long insulin analogue. *Diabetol. Metab. Syndr.* **2015**, 7:57.

[45] Bhattacharya, A. A.; Grüne, T.; Curry, S. Crystallographic analysis reveals common modes of binding of medium and long-chain fatty acids to human serum albumin. *J. Mol. Biol.* **2000**, *303*, 721-732.

[46] Mariam, J.; Sivakami, S.; Dongre, P. M. Albumin corona on nanoparticles - a strategic approach in drug delivery. *Drug Dliv.* **2016**, *23*, 2668-2676.

[47] Torchilin, V. P.; Berdichevsky, V. R.; Barsukov, A. A.; Smirnov, V. N. Coating liposomes with protein decreases their capture by macrophages. *FEBS Lett.* **1980**, *111*, 184-188.

[48] Yokoe, J.; Sakuragi, S.; Yamamoto, K.; Teragaki, T.; Ogawara, K.; Higaki, K.; Katayama, N.; Kai, T.; Sato, M.; Kimura, T. Albumin-conjugated PEG liposome enhances tumor distribution of liposomal doxorubicin in rats. *Int. J. Pharm.* **2008**, *353*, 28-34.

[49] Furumoto, K.; Yokoe, J.; Ogawara, K.; Amano, S.; Takaguchi, M.; Higaki, K.; Kai, T.; Kimura, T. Effect of coupling of albumin onto surface of PEG liposome on its in vivo disposition. *Int. J. Pharm.* **2007**, *329*, 110-116.

[50] Vuarchey, C.; Kumar, S.; Schwendener, R. Albumin coated liposomes: a novel platform for macrophage specific drug delivery. *Nanotechnol. Devel.* **2011**, *1*, e2.

[51] Hansen, M. B.; van Gaal, E.; Minten, I.; Storm, G.; van Hest, J. C. M.; Löwik, D. W. P. M. Constrained and UV-activatable Cell-penetrating Peptides for Intracellular Delivery of Liposomes. *J. Control. Release* **2012**, *164*, 87-94.

[52] Sumbayev, V. V.; Ysinska, I. M.; Garcia, C. P.; Gilliland, D.; Lall, G. S.; Gibbs, B. F.; Bonsall, D. R.; Varani, L.; Rossi, F.; Calzolai, L. Gold nanoparticles downregulate interleukin-1β-induced pro-inflammatory responses. *Small* **2013**, *9*, 472-477.

[53] Schnyder, A.; Krähenbühl, S.; Török, M.; Drewe, J.; Huwyler, J. Targeting of skeletal muscle in vitro using biotinylated immunoliposomes. *Biochem. J.* **2004**, *377*, 61-67.

[54] Huy, T. Q.; Chung, P. V.; Thuy, N. T.; Blanco-Andujar, C.; Thanh, N. T. Protein A-conjugated iron oxide nanoparticles for separation of Vibrio cholerae from water samples. *Faraday Discuss.* **2014**, *175*, 73-82.

[55] Varshney, M.; Yang, L.; Su, X. L.; Li, Y. Magnetic nanoparticle-antibody conjugates for the separation of Escherichia coli O157:H7 in ground beef. *J. Food Prot.* **2005**, *68*, 1804-1811.

CHAPTER 2

Bilirubin-Mediated Coating of Liposome with Serum Albumin

Reproduced with permission from Sato, H.; Nakamura, Y.; Nakhaei, E.; Funamoto, D.; Kim, C. W.; Yamamoto, T.; Kishimura, A.; Mori, T.; Katayama, Y. A liposome reversibly coated with serum albumin. *Chemistry Letters* **2014**, *43*, 1481-1483. Copyright 2014 The Chemical Society of Japan.

2.1. Introduction

Human serum albumin (HSA) is a weakly acidic protein (isoelectric point, pI 4.9), which exists in plasma at a relatively high concentration of ~40 mg/mL (~0.6 mM) [1]. Because HSA is a hydrophilic protein and is not immunogenic, surface coating of solid materials with HSA is known to suppress non-specific adsorption of blood proteins, as well as prevent recognition of the materials by antibodies and complements to improve biocompatibility [2-4]. Because bovine serum albumin (BSA) has similar physicochemical properties to HSA and 76 % amino acid sequence homology with HSA, BSA can also be used for surface coating. Coating a material surface with serum albumin is usually achieved through covalent bonding or physical adsorption. Covalent bonding enables formation of a stable coating layer of serum albumin [2–4], although it does not allow for spontaneous exchange with fresh serum albumin. Coating using physical adsorption via electrostatic or hydrophobic interaction is reversible and makes the serum albumin exchange reaction possible [5–7], however in some cases, it can cause denaturation of the serum albumin [6,7].

On the other hand, coating a material surface by using specific interactions between ligands and serum albumin is reversible but results in stable coatings, and is

expected to maintain the intact conformation of serum albumin and circumvent the disadvantages of both covalent and physical adsorption. Serum albumin has flexible structure and provide inner hydrophobic binding site for bilirubin, long-fatty acid, and hormones. The interaction between such ligands and serum albumin pockets have been extensively investigated, and binding affinity of the ligands are known to be quite strong (e.g. K_d = 20 nM for bilirubin and K_d = 1.4 - 100 nM for long- fatty acids) [8,9]. Surface coating using the specific interaction between these pockets and alkyl ligands is therefore more favorable than non-specific physical interaction because the binding affinity is relatively strong [10-13] whilst allowing HSA to maintain a native conformation.

Surface coating of polymer nanoparticles, inorganic materials, and liposomes with HSA is also useful because it prevents recognition by antibodies and complements, as well as improving colloidal stability to extend blood circulation time [14]. To coat the surface of nanoparticles, covalent bonding or nonspecific physical interaction have so far been used [14], and surface coating of nanoparticles via the specific interaction of HSA hydrophobic pockets and ligands is less common [15]. There are several reports of HSA coating of liposomes via covalent bonding [16-19], but none reporting liposome coating via specific hydrophobic interaction with alkyl ligands. Here, I report coating of the liposome surface via serum albumin using albumin-specific ligand (**Figure 2.1**). As such ligand, I selected bilirubin, which is known to strongly but reversibly bind to sub-domain IB of serum albumin (**Figure 2.2a**) [1]. The one carboxyl group of bilirubin is exposed from the pocket (**Figure 2.2b,c**) [20]. To facilitate the incorporation of bilirubin into the pocket, bilirubin was attached to the terminus of PEG (M_n = 2000)-modified phosphatidylethanolamine (**1**) through its one carboxylate (**Scheme 2.1**). In this study, BSA was used instead of HSA because of the high homology to HSA and the low cost.

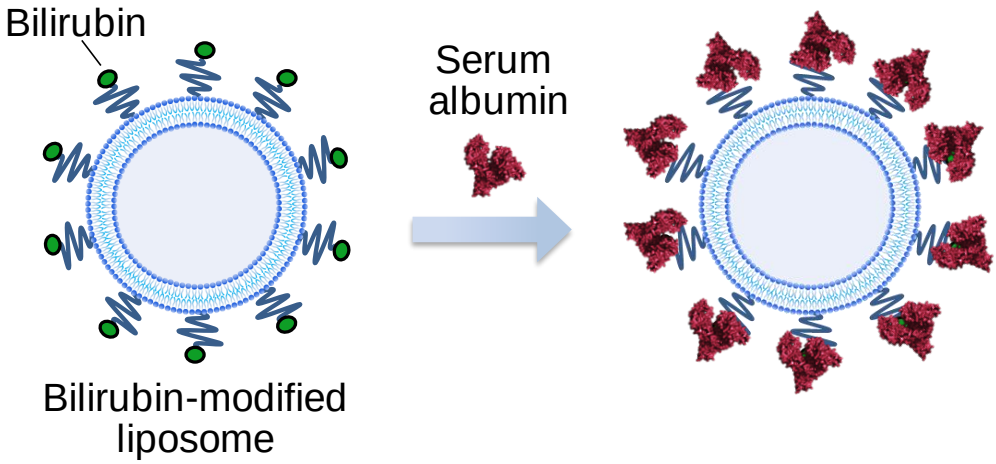

Figure 2.1 Schematic illustration of the present serum albumin-coated liposome.

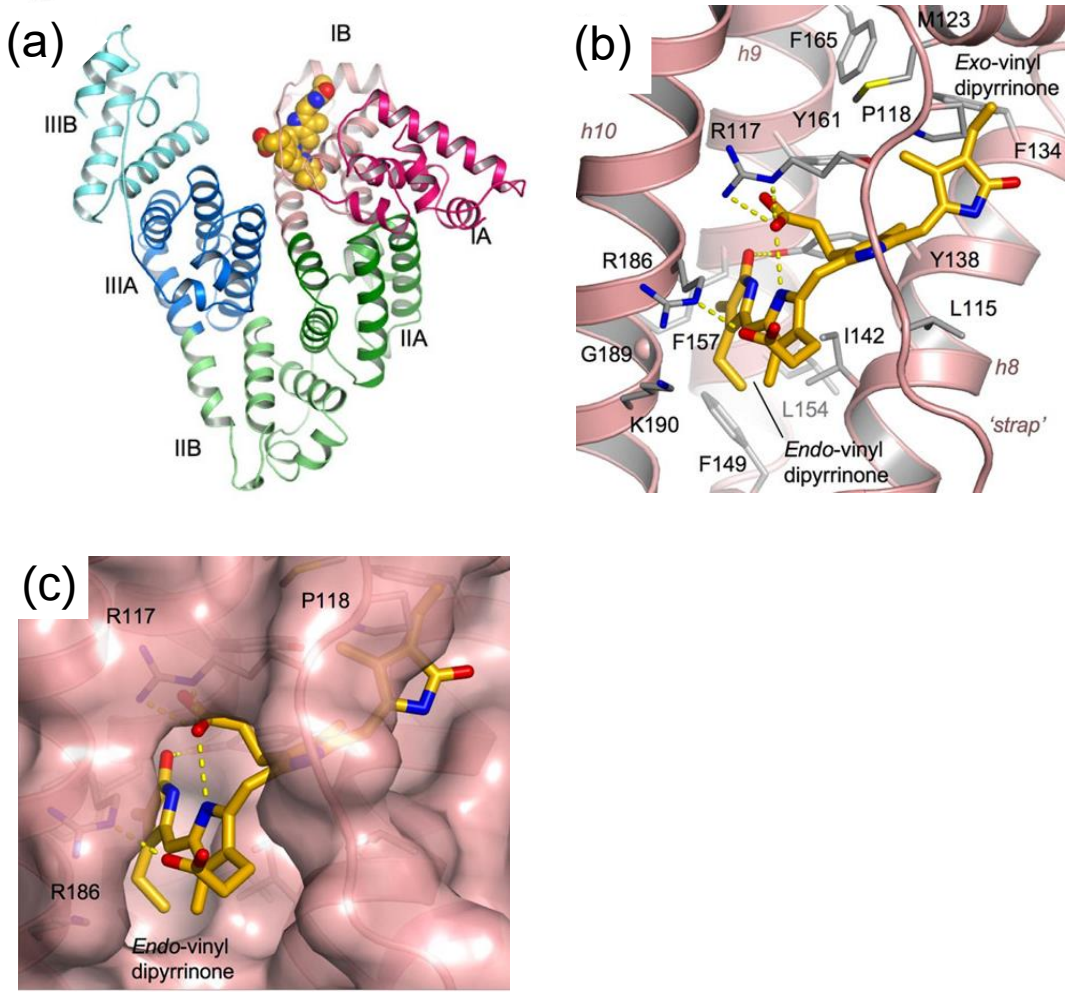

Figure 2.2. (a) HSA complexed with bilirubin. (b) Detailed view of the interaction between bilirubin and binding pocket in sub-domain IB. The broken yellow lines show the hydrogen bonds. The grey sticks show the albumin amino acid side chain. (c) View of the fit of bilirubin to the binding pockets in sub-domain IB [20]. © 2008 Elsevier Ltd.

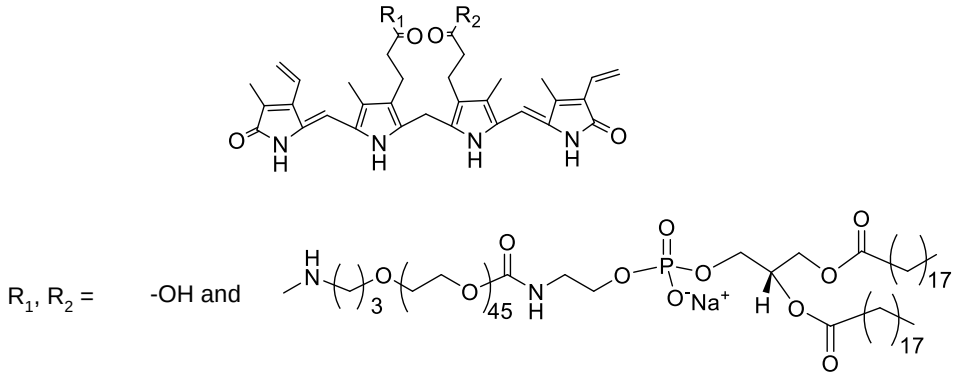

Scheme 2.1. Chemical structure of bilirubin-modified lipid **1**. © 2014 The Chemical Society of Japan.

2.2. Materials and Methods

2.2.1. Materials.

N-(aminopropyl polyethyleneglycol) carbamyl-distearoylphosphatidyl-ethanolamine (PEG, Mn = 2000) (DSPE-PEG2000-NH2) was purchased from NOF. Diphenylphosphoryl azide (DPPA) and triethylamine, dry DMSO, and chloroform were purchased from Wako Pure Chemical Industries. Bilirubin was purchased from Tokyo Chemical Industry. Bovine serum albumin (BSA, fatty acid free) was purchased from Sigma-Aldrich. Fluorescein-labeled BSA (0.68 fluorescein/BSA) was prepared with fluorescein-5-maleimide (Molecular Probes). DiD (DiIC18(5)) was purchased from PromoKine.

2.2.2. Synthesis of N-(aminopropyl polyethyleneglycol) carbamyl-distearoylphosphatidyl-ethanolamine-bilirubin (**1**).

In a test tube, bilirubin (20 mg, 35 μmol), DPPA (75 μL, 0.35 mmol) and 1 mL of triethylamine (50 μL, 0.36 mmol) was dissolved with dry DMSO (5 mL). Then, to the mixture, dry DMSO solution (1 mL) of DSPE-PEG2000 (23 mg, 8.1 μmol) was added dropwise, and the mixture was stirred overnight. Further diphenylphosphoryl azide (75 μL, 0.35 mmol) was added to the mixture and stirred for 2 h at 50 ℃. The crude compound was purified by dialysis with Spectra/Por® 6 membrane (MWCO 1000) against DMSO for 4 days then chloroform for 1 day, and evaporated. ^{1}H-NMR (300 MHz, $CDCl_3$): δ 0.89 (t, CH_3, 6H); 1.3 (m, CH_2, 56H); 3.4 (m, OCH_2CH_2NHCO,2H); 3.6-4.4 (m, PEG, ≈180H and C=C(NH)CH_2C(NH)=C, 2H); 5.2-6.6 (m, protons of bilirubin, 8H)

2.2.3. Preparation of liposome modified with lipid **1**.

Lipid hydration was used for the preparation of the liposomes. A chloroform solution of DSPC, cholesterol, DSPE-PEG_{2k}, and **1** [55: 45: 5] was mixed in a round bottom flask. Chloroform was removed by evaporation at 65 ℃ to form a thin film of lipid mixture. Traces of organic solvent were removed by keeping the film under vacuum for at least 2 h. The lipid film was hydrated with 3 mL of PBS/NaOHaq (pH 9.0), followed by heating in a water bath at 65 ℃, and vortexing for 10 min. The heat and vortex cycle was repeated 10 times. The lipid suspension was sequentially extruded (Avanti Polar Lipids, Alabaster, AL, U.S.A.) through polycarbonate membranes of 200 nm pore size. The extrusion was performed at 65 ℃ and repeated 21 times. To label the liposome with DiD, 3 mol% of DiD was mixed with lipids when preparing the lipid membrane.

2.2.4. Measurement of the diameter.

The PBS/NaOHaq solution (20 μL, pH 9.0) of **1** (18 μM) was added to the PBS solution (0.18 mL) of BSA (0.15 mM), and the mixture was incubated for 15 min at room temperature. The hydrodynamic diameter of the liposomes was measured using a Malvern Zetasizer Nano ZS (Worcestershire, U.K.).

2.2.5. Gel filtration chromatography.

A 50-μL of liposome solution including 7.5 nmol of **1** [in PBS/NaOHaq (pH 9.0)] was mixed with a 50 μL of fluorescein-labeled BSA (77 nmol). Then, the mixture was incubated for 15 min at room temperature for complex formation. Then, the liposome/BSA mixture was applied to a Sephadex G-100 column and the eluted solution was fractionated by every 330 μL. The absorbance of each fractions were measured at 416.5 nm and 494 nm, respectively. BSA alone (7.6 nmol/50 μL of PBS)

was also analyzed by the column.

2.2.6. Determination of BSA amount covering the liposome and control liposome.

A 50 μL of liposome solution containing 23 nmol of **1** [in HEPES/NaOHaq (pH 8.7)] or control liposome solution (prepared without **1**) [in HEPES (pH 7.4)] were mixed with a 10 μL of fluorescein-labeled BSA (15 nmol), respectively. Then, the mixtures were incubated for 3 h at room temperature for complex formation. Then, 300 μL of 10 mM HEPES was added to each mixture and the solutions were ultrafiltrated using Vivaspin tube (MWCO 300,000). To the residual solutions, 200 μL of 10 mM HEPES was added for dilution. The fluorescence of each solution was measured at 649 nm (DiD) and 494 nm (fluorescein), respectively.

2.2.7. Confirmation of reversibility of albumin binding with liposome.

A 50-μL of liposome solution containing 23 nmol of **1** [in HEPES/NaOHaq (pH 8.7)] was mixed with a 10 μL of fluorescein-labeled BSA (15 nmol) and incubated for 1.5 h at room temperature. Then, a 400 μL of 10 mM HEPES solution containing non-fluorescence-labeled BSA (138 nmol) was added to the solution and incubated for further 4 h at room temperature. Then, the solution was ultrafiltrated using Vivaspin tube (MWCO 300,000). To the residual solutions, 200 μL of 10 mM HEPES was added for dilution. The fluorescence of each solution was measured at 494 nm (fluorescein) and 494 nm (DiD), respectively.

2.3. Results and Discussions

2.3.1. Preparation of **1**.

The bilirubin-modified lipid **1** was synthesized as described in **Scheme 2.2**. Bilirubin was modified onto the amine group at the terminus of PEG (Mn = 2000)-modified phosphatidylethanolamine by using a condensing reagent of diphenylphosphoryl azide. One of the two carboxyl groups included in bilirubin was used for the reaction. After the reaction, unreacted bilirubin was removed by dialysis to obtain lipid **1**. The modification ratio of bilirubin on the terminal amine group of the lipid was determined by ^{1}H NMR to be 96%, implying almost quantitative modification of the lipid with bilirubin (**Figure 2.3**). **Figure 2.4** shows the UV spectra of **1** and free bilirubin dissolved in chloroform and DMSO, respectively. Comparing with free bilirubin, the bilirubin unit of **1** showed blue shift. This blue shift may be ascribed to the isomerization of the bilirubin unit of **1** into 4Z,15E-form [21,22]. Free bilirubin usually has 4Z,15Z-form due to the intramolecular hydrogen bonding [23,24]. It was reported that 4Z,15Z-bilirubin requires photoinduced isomerization to change the conformation to 4Z,15E-form for binding with serum albumin [20]. In contrast, lipid **1** may stably exists as 4Z,15E-form to be ready to bind to serum albumin. This will be an advantageous characteristic of **1** as a ligand for serum albumin.

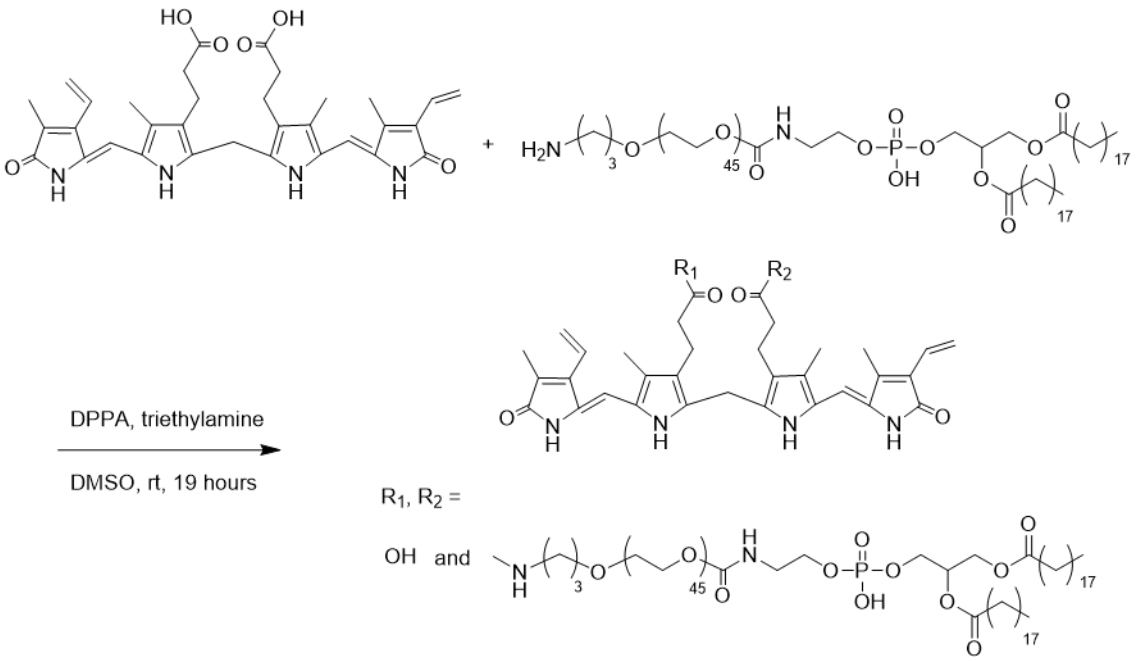

Scheme 2.2. Synthesis of lipid **1**. © 2014 The Chemical Society of Japan.

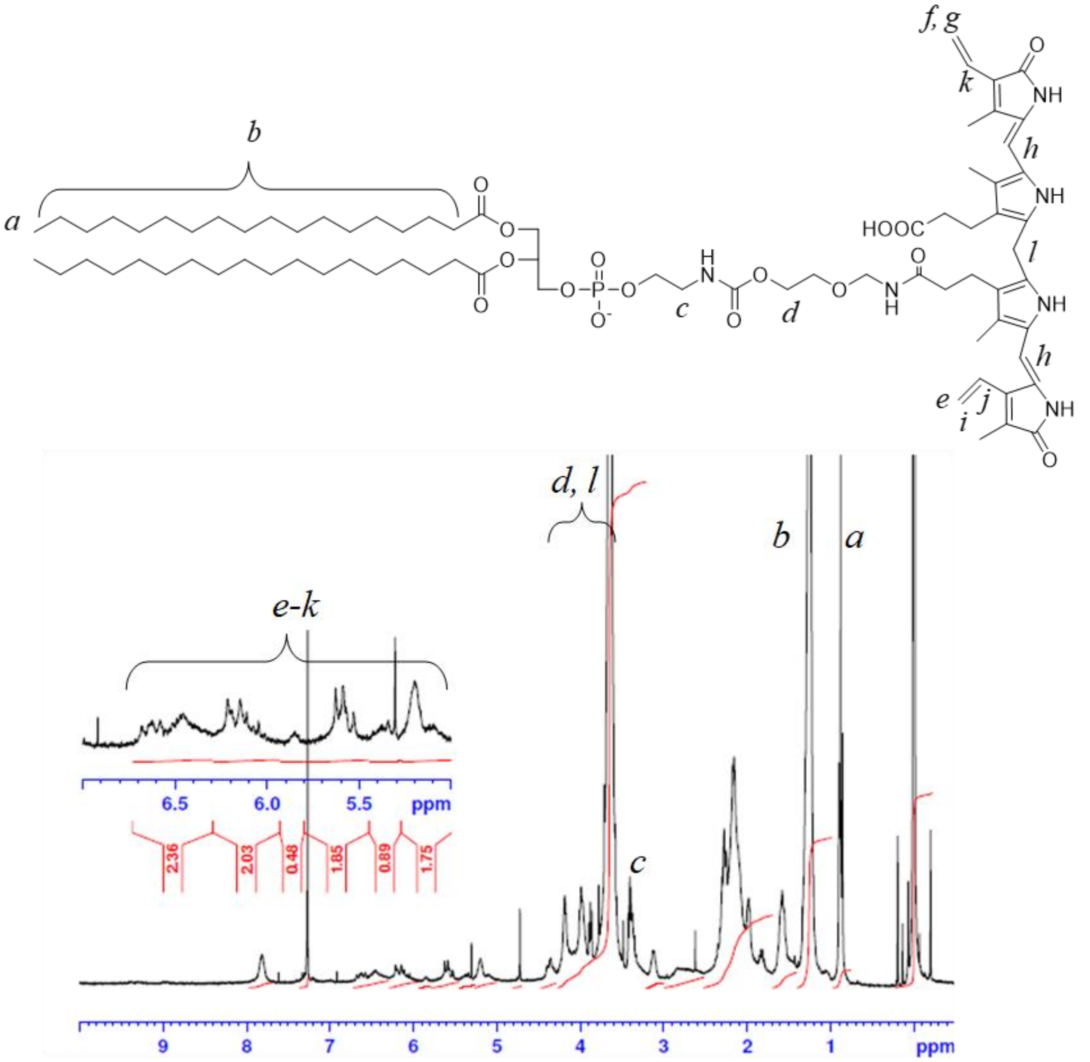

Figure 2.3. ^{1}H NMR spectrum of lipid **1** (300 MHz, in $CDCl_3$). © 2014 The Chemical Society of Japan.

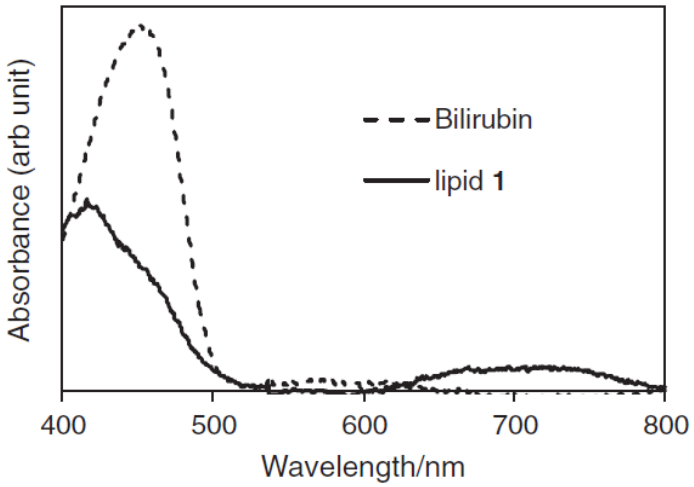

Figure 2.4. Absorption spectra of **1** and free bilirubin. Concentration of bilirubin was 0.86 μM. © 2014 The Chemical Society of Japan.

2.3.2. Characteristics of liposome.

Liposome-containing lipid **1** was prepared by a hydration method. Briefly, chloroform solution of 1,2-distearoyl-snglycero-3-phosphocholine (DSPC): cholesterol:**1** = 55:45:5 was dried *in vaccuo* to prepare a thin film on the surface of the pear-shaped flask. The obtained film was hydrated by a slightly alkaline buffer solution (pH 9.0) because of the good solubility of lipid **1** in the slightly alkaline condition. After the dissolution of the film, the obtained dispersion was passed through a 200 nm-pore extruder. The obtained liposome was diluted with PBS (pH 7.5). Then, the liposome was mixed with 0.13 mM of bovine serum albumin (BSA) for complexation between the bilirubin on the liposome surface and BSA. **Figure 2.5** shows the diameter distribution of the original liposome and the liposome mixed with BSA. A slight increase of the diameter from 200.4 ± 1.0 to 233.3 ± 3.4 nm was observed by mixing with BSA. This increase seemed to reflect the complexation of BSA with bilirubin on the liposome surface. The size distribution was not changed for the examined time span (up to 12 h).

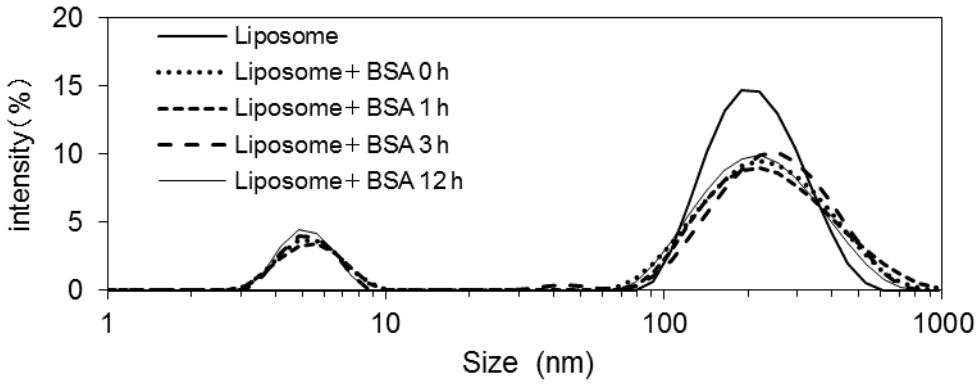

Figure 2.5. Time-dependence of size-distribution of bilirubin-modified liposome in the presence of 0.14 mM BSA in HEPES (pH 7.4). Concentration of **1** was 15 μM. A component with a small diameter (< 10 nm) is BSA. © 2014 The Chemical Society of Japan.

2.3.3. Confirmation of BSA coating of liposome.

To obtain further evidence of the BSA modification, the BSA/iposome mixture was analyzed by a gel filtration chromatography with a Sephadex G-100 column (**Figure 2.6**). First, the elution profile of a fluorescein-labeled BSA was measured. The fluorescein-labeled BSA was eluted from 6 to 13 mL. Then, the elution profile of the fluorescein-labeled BSA-liposome mixture was monitored at two different wavelengths, 416.5 and 494 nm, which correspond to maximum wavelength of bilirubin and fluorescein, respectively. As a result, the elution of the liposome was started from 5 mL, which corresponds to an exclusion volume of this column. Meanwhile, BSA was eluted in a wide range that includes the elution volume of the liposome. These results clearly indicate the binding of BSA to bilirubin on the liposome surface.

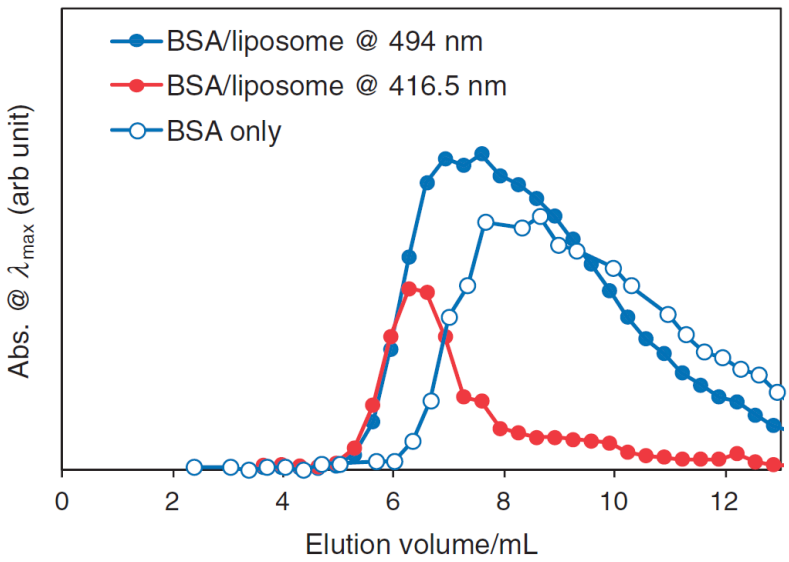

Figure 2.6. Elution profiles of fluorescein-labeled BSA-liposome mixture monitored at 416.5 and 494 nm, which correspond to λ_{max} of bilirubin and fluorescein, respectively. The elution profile of the fluorescein-labeled BSA alone was also measured for comparison. © 2014 The Chemical Society of Japan.

2.3.4. Determination of BSA amount coating the liposome and control liposome.

The binding ratio of bilirubin with fluorescein-labeled BSA was determined after isolating the fluorescein-labeled BSA/liposome complex with ultrafiltration (**Figure 2.7**). It was found that about 21% of bilirubin on the liposome bind with BSA. This relatively low binding ratio may result from the hydrophobic nature of bilirubin. The bilirubin group of lipid **1** may be buried into the liposome membrane, leading to less chances of binding with BSA.

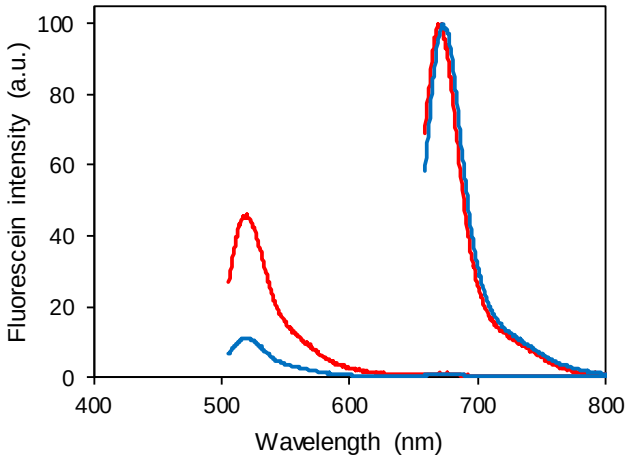

Figure 2.7. Fluorescence spectra of complex between fluorescein-labeled BSA and bilirubin-modified liposome (red line) or control liposome (blue line). Fluorescein (Ex. at 494 nm) and DiD (Ex. at 649 nm). The complex was isolated by ultrafiltration. © 2014 The Chemical Society of Japan.

2.3.5. Confirmation of reversibility in albumin binding with liposome.

I examined the reversibility of the bilirubin binding to BSA. After biding of the liposome with fluorescein-labeled BSA, the 10-times excess amount of non-labeled BSA was added to compete with the bound fluorescein-labeled BSA. Then, the BSA/liposome complex was isolated by ultrafiltration. As a result, the remaining fluorescein was almost diminished after the addition of non-labeled BSA (**Figure 2.8**), indicating the replacement of fluorescein-labeled BSA bound to liposome with non-labeled BSA. Thus, it can be concluded that the binding of BSA to liposome is reversible.

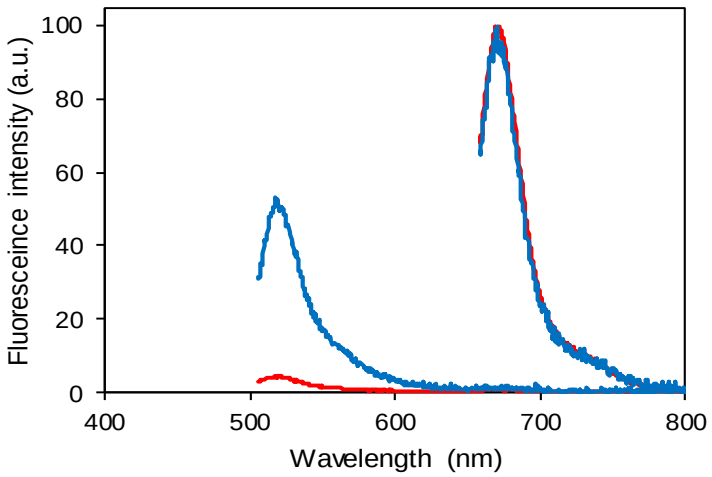

Figure 2.8. Fluorescence spectra of complex between BSA and bilirubin-modified liposome. Liposome was first complexed with fluorescein-labeled BSA (blue line). To the complex, the 10-times excess amount of non-labeled BSA was added for replacement (red line). Fluorescein (Ex. at 494 nm) and DiD (Ex. at 649 nm). © 2014 The Chemical Society of Japan.

2.4. Conclusions

I proposed here a reversible noncovalent coating of serum albumin on the liposome surface. The liposome includes a lipid modified with a specific ligand for serum albumin, bilirubin. The conformation of bilirubin of the lipid was indicated to be 4Z,15E-form, which is suited for the binding to serum albumin. The coating of the liposome surface with bovine serum albumin was supported by a gel filtration chromatography. I believe that the liposome presented here will be applicable to a drug carrier with extended blood circulation time due to the nonimmunogenic and endosomal recycling characteristics of serum albumin.

2.5. References

[1] Peters, T., Jr. *All about Albumin: Biochemistry, Genetics and Medical Applications*; Academic Press, Inc.: Orlando, FL, 1996.

[2] An, Y. H.; Stuart, G. W.; McDowell, S. J.; McDaniel, S. E.; Kang, Q.; Friedman, R. J. Prevention of bacterial adherence to implant surfaces with a crosslinked albumin coating in vitro. *J. Orthopaedic Res.* **1996**, *14*, 846-849.

[3] Steffens, G. C. M.; Nothdurft, L.; Buse, G.; Thissen, H.; Hocker, H.; Klee, D. High density binding of proteins and peptides to poly(D,L-lactide) grafted with polyacrylic acid. *Biomaterials* **2002**, *23*, 3523-3531.

[4] Ulbricht, M.; Riedel, M. Ultrafiltration membrane surfaces with grafted polymer 'tentacles': preparation, characterization and application for covalent protein binding. *Biomaterials* **1998**, *19*, 1229-1237.

[5] Jeyachandran, Y. L.; Mielczarski, E.; Rai, B.; Mielczarski, J. A. Quantitative and qualitative evaluation of adsorption/desorption of bovine serum albumin on hydrophilic and hydrophobic surfaces. *Langmuir* **2009**, *19*, 11614-11620.

[6] Vermonden, T.; Giacomelli, C. E.; Norde, W. Reversibility of structural rearrangements in bovine serum albumin during homomolecular exchange from AgI particles. *Langmuir* **2001**, *17*, 3734-3740.

[7] Norde, W.; Giacomelli, C. E. BSA structural changes during homomolecular exchange between the adsorbed and the dissolved states. *J. Biotechnol.* **2000**, *79*, 259-268.

[8] Weisiger, R. A.; Ostrow, J. D.; Koehler, R. K.; Webster, C. C.; Mukerjee, P.; Pascolo, L.; Tiribelli, C. Affinity of human serum albumin for bilirubin varies with albumin concentration and buffer composition. *J. Biol. Chem*. **2001**, *276*, 29953-29960.

[9] Richieri, G. V.; Anel, A.; Kleinfeld, A. M. Interactions of Long-chain Fatty Acids and Albumin: Determination of Free Fatty Acid Levels using the Fluorescent Probe ADIFAB. *Biochemistry* **1993**, *32*, 7574-7580.

[10] Eberhart, R. C.; Munro, M. S.; Williams, G. B.; Kulkarni, P. V.; Shannon, W. A. Jr.; Brink, B. E.; Fry, W. J. Albumin adsorption and retention on C18-alkyl-derivatized polyurethane vascular grafts. *Artif. Organs*. **1987**, *11*, 375-382.

[11] Pitt, W. G.; Cooper, S. L. Albumin adsorption on alkyl chain derivatized polyurethanes: I. The effect of C-18 alkylation. *J. Biomed. Mater. Res*. **1988**, *22*, 359-382.

[12] Pitt, W. G.; Grasel, T. G.; Cooper, S. L. Albumin adsorption on alkyl chain derivatized polyurethanes. II. The effect of alkyl chain length. *Biomaterials* **1988**, *9*, 36-46.

[13] Wang, D.; Ji, J.; Gao, C.; Yu, G.; Feng, L. Surface coating of stearyl poly(ethylene oxide) Coupling-polymer on polyurethane guiding catheters with poly(ether urethane) film-building additive for biomedical applications. *Biomaterials* **2001**, *22*, 1549-1562.

[14] Mariam, J.; Sivakami, S.; Dongre, P. M. Albumin corona on nanoparticles - a strategic approach in drug delivery. *Drug Dliv.* **2016**, *23*, 2668-2676.

[15] Nakamura, Y.; Sato, H.; Nobori, T.; Matsumoto, H.; Toyama, S.; Shuno, T.; Kishimura, A.; Mori, T.; Katayama, Y. Modification of ligands for serum albumin on polyethyleneimine to stabilize polyplexes in gene delivery. *J. Biomater. Sci. Polym. Ed.* **2017**, *28*, 1382-1393.

[16] Torchilin, V. P.; Berdichevsky, V. R.; Barsukov, A. A.; Smirnov, V. N. Coating Liposomes with protein decreases their capture by macrophages. *FEBS Lett.* **1980**, *111*, 184-188.

[17] Yokoe, J.; Sakuragi, S.; Yamamoto, K.; Teragaki, T.; Ogawara, K.; Higaki, K.; Katayama, N.; Kai, T.; Sato, M.; Kimura, T. Albumin-conjugated PEG liposome enhances tumor distribution of liposomal doxorubicin in rats. *Int. J. Pharm.* **2008**, *353*, 28-34.

[18] Furumoto, K.; Yokoe, J.; Ogawara, K.; Amano, S.; Takaguchi, M.; Higaki, K.; Kai, T.; Kimura, T. Effect of coupling of albumin onto surface of PEG liposome on its in vivo disposition. *Int. J. Pharm.* **2007**, *329*, 110-116.

[19] Vuarchey, C.; Kumar, S.; Schwendener, R. Albumin coated liposomes: a novel platform for macrophage specific drug delivery. *Nanotechnol. Devel.* **2011**, *1*, e2.

[20] Zunszain, P. A.; Ghuman, J.; McDonagh, A. F.; Curry, S. Crystallographic analysis of human serum albumin complexed with 4Z,15E-bilirubin-IXalpha. *J. Mol. Biol.* **2008**, *381*, 394-406.

[21] Plavskii, V. Y.; Mostovnikov, V. A.; Tret'yakova, A. I.; Mostovnikova, G. R. Sensitizing effect of Z,Z-bilirubin IXα and its photoproducts on enzymes in model solutions. *J. Appl. Spectrosc.* **2008**, *75*, 407-419.

[22] McDonagh, A. F.; Agati, G.; Fusi, F.; Pratesi, R. Quantum yields for laser photocyclization of bilirubin in the presence of human serum albumin. Dependence of quantum yield on excitation wavelength. *Photochem. Photobiol*. **1989**, *50*, 305-319.

[23] Onishi, S.; Miura, I.; Isobe, K.; Itoh, S.; Ogino, T.; Yokoyama, T.; Yamakawa, T. Structure and thermal interconversion of cyclobilirubin IX α. *Biochem. J.* **1984**, *218*, 667-676.

[24] Iwase, T.; Kusaka, T.; Itoh, S. (EZ)-Cyclobilirubin formation from bilirubin in complex with serum albumin derived from various species. *J. Photochem. Photobiol. B* **2010**, *98*, 138-143.

CHAPTER 3

Alkyl Chain-Mediated Coating Liposomes with Serum Albumin

3.1. Introduction

In Chapter 2, I developed the first type of ligand-modified liposome for coating with serum albumin using bilirubin as a specific ligand. The liposome was successfully coated with serum albumin. However, the liposome showed relatively low binding ratio (~21%), which may result from the hydrophobic nature of bilirubin. Hydration of dried membrane was low, and the bilirubin might be buried into the liposome membrane [1], leading to less chances of binding. Therefore, I exploited a new type of ligand-modified liposome, which is readily soluble in aqueous solution with exposing ligand to an aqueous phase. Here I present the alkyl chain-mediated strategy for coating liposome surfaces with human serum albumin (HSA). As shown in **Figure 3.1A**, HSA has seven hydrophobic pockets for specific binding with relatively long fatty acids such as palmitic acid and stearic acid. A cationic amino acid (lysine or arginine) is located at the bottom of these pockets, to enhance the binding affinity via electrostatic interaction with the anionic carboxylate of the fatty acids [2-4]. The binding affinities of the fatty acids with these pockets are quite strong; the dissociation constant (K_d) for stearic acid with the strongest pocket is ~10^{-9} M [5]. The specific interaction between these pockets and alkyl ligands has been used for the surface

coating of polyurethane-based implants [6-8] and catheters [9]. However, alkyl ligands-mediated coating of liposome with HSA has not been reported. This is due to the difficulty associated with exposing the hydrophobic alkyl ligands to an aqueous phase prior to HSA binding (**Figure 3.1B**). Here I established conditions to enable the handling of alkyl ligands in an aqueous phase and achieved coating of liposome surfaces with HSA via the ligands.

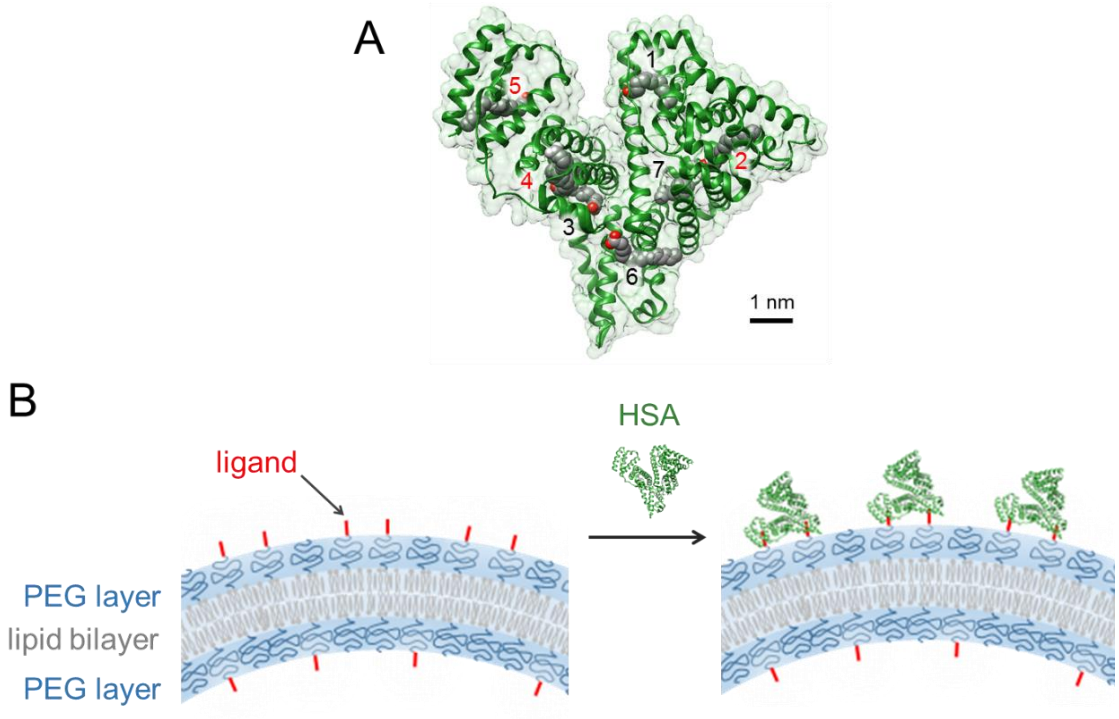

Figure 3.1 (A) Crystal structure of HSA bound to seven stearic acid molecules (PDB ID: 1E7I). Numbers show pockets that bind with stearic acids. Numbers shown in red are strong binding pockets [4]. (B) Schematic representation of ligand-mediated coating of HSA on PEGylated liposome surface. Hydrophobic ligands must be exposed on the surface prior to coating with HSA. © 2018 American Chemical Society.

3.2. Materials and Methods

3.2.1. Materials.

Octadecanedioic acid, decanoic acid, N-ethylmaleimide and cholesterol were purchased from Tokyo Chemical Industry (Tokyo, Japan). Water-soluble carbodiimide (WSC) was purchased from Dojindo (Kumamoto, Japan). N-(aminopropyl polyethyleneglycol)carbamyl-distearoylphosphatidyl-ethanolamine (DSPE-PEG$_{2k}$-NH$_2$), N-(Carbonyl-methoxypolyethyleneglycol 2k)-1,2-distearoyl-sn-glycero-3-phosphoethanolamine, sodium salt (DSPE-PEG$_{2k}$), 1,2-distearoyl-sn-glycero-3-phosphocholine (DSPC), N-[(3-Maleimide-1-oxopropyl)aminopropyl polyethyleneglycol-carbamyl] distearoylphosphatidyl-ethanolamine (DSPE-PEG$_{2k}$-Mal), and 1,2-dipalmitoyl-sn-glycero-3-phosphocholine were purchased from NOF corporation (Tokyo, Japan). Stearic acid, albumin from human serum (HSA, lyophilized powder, essentially fatty acid free), N-hydroxysuccinimide (NHS), transferrin human, and albumin from chicken egg white (ovalbumin) were purchased from Sigma-Aldrich (St. Louis, MO, U.S.A.). Maleic anhydride was purchased from Kishida Chemical (Osaka, Japan). Dulbecco's Modified Eagle's medium (DMEM) was purchased from Wako Pure Chemical Industries (Tokyo, Japan). AIM-V medium was purchased from Invitrogen (Carlsbad, U.S.A).

3.2.2. Synthesis of decanoate-modified DSPE-PEG$_{2k}$ (**1**).

Decanoic acid (3.8 mg, 22.1 μmol), N-hydroxysuccineimide (7.8 mg, 67.8 μmol), WSC (12.3 mg, 64.2 μmol) and triethylamine (20 μL, 138.5 μmol) were dissolved in 1 mL of super dehydrated chloroform and the mixture was stirred at room temperature for 40 min. Subsequently, 1 mL of chloroform containing

DSPE-PEG$_{2k}$-NH$_2$ (50 mg, 18 μmol) was added to the mixture. The mixture was then allowed to react for 27 h at room temperature. The product was purified by dialysis using Spectra/Por® 6 membrane (MWCO 1000) against chloroform and methanol for 6 days. Finally, the dry product (15.5 mg, 5.3 μmol, 29%) was obtained by evaporating the solvent. ^{1}H NMR (400 MHz, MeOD): δ 0.90 (t, CH_3, 9H); 1.29 (s, CH_2, 68H); 1.59 (m, C*H*$_2$CH$_2$CO, 6H); 1.75 (m, C*H*$_2$CH$_2$CONH, 2H); 2.16 (m, C*H*$_2$CONH, 2H); 2.32 (m, CH_2CO, 6H); 3.64 (s, PEG, ≈180H); 5.22 (s, PO$_4$CH$_2$C*H*CH$_2$OCO, 1H).

3.2.3. Synthesis of stearate-modified DSPE-PEG$_{2k}$ (**2**).

2 was obtained similarly to 1 using stearic acid. ^{1}H NMR (400 MHz, MeOD): δ 0.90 (t, CH_3, 9H); 1.29 (s, CH_2, 84H); 1.60 (m, C*H*$_2$CH$_2$CO, 6H); 1.75 (m, C*H*$_2$CH$_2$CONH, 2H); 2.17 (t, C*H*$_2$CONH, 2H); 2.33 (m, CH_2CO, 6H); 3.63 (s, PEG, ≈180H); 5.22 (s, PO$_4$CH$_2$C*H*CH$_2$OCO, 1H).

3.2.4. Synthesis of octadencanedioete-modified DSPE-PEG$_{2k}$ (**3**).

3.2.4.1. Synthesis of mono-NHS ester of octadecanedioic acid.

Octadecanedioic acid (471mg, 1.5 mmol) and N-hydroxysuccinimide (10 mg, 2.3 mmol) were dissolved in 6 mL of N,N-dimethylformamide which was kept at 50 °C. A solution of WSC (462 mg, 2.1 mmol) in 4.3 mL of N,N-dimethylformamide was added dropwise, and the reaction mixture was stirred at 50°C for 3 h. The solution was washed with saturated NH_4Cl solution and extracted with diethylether. The organic layer was evaporated to yield the desired product (211 mg, 0.51 mmol, 34%). ^{1}H NMR (300 MHz, MeOD): δ 1.29 (m, CH_2, 24H), 1.59 (m, C*H*$_2$CH$_2$COOH, 2H), 1.72 (m, C*H*$_2$CH$_2$COON, 2H), 2.27 (t, C*H*$_2$COOH, 2H), 2.61 (t, C*H*$_2$COON, 2H), 2.83 (s, COC*H*$_2$C*H*$_2$CO, 4H).

3.2.4.2. Coupling of mono-NHS ester of octadecanedioic acid and DSPE-PEG_{2k}-NH_2.

Mono-NHS ester of octadecanedioic acid (2.5 mg, 6.2 μmol) and DSPE-PEG_{2k}-NH_2 (9.9 mg, 3.6 μmol) were dissolved in 600 μL of chloroform containing 120 mM triethylamine, and the mixture was stirred for 6 h at room temperature. The product was purified by dialysis using Spectra/Por® 6 membrane (MWCO 1000) against chloroform and methanol for 4 days. Finally, the dry product (7.9 mg, 2.6 μmol, 71%) was obtained by evaporating the solvent. ^{1}H NMR (300 MHz, MeOD): δ 0.90 (t, CH_3, 9H); 1.29 (s, CH_2, 68H); 1.59 (m, C*H*$_2$$CH_2CO$, 6H); 1.71-1.79 (quintet, C*H*$_2$$CH_2CONH$, 2H.); 2.17 (t, C*H*$_2$CONH, 2H); 2.25-2.37 (m, C*H*$_2$CO, 6H); 3.64 (s, PEG, ≈180H); 5.22 (s, $PO_4CH_2CHCH_2OCO$, 1H).

3.2.5. Preparation of liposomes.

Lipid hydration was used for the preparation of the liposomes. A chloroform solution of DSPC, cholesterol, DSPE-PEG_{2k}, and ligand-modified lipid [56: 39: (5-x): x (mol%)] was mixed in a round bottom flask. Chloroform was removed by evaporation at 65 °C to form a thin film of lipid mixture. Traces of organic solvent were removed by keeping the film under vacuum for at least 2 h. The lipid film was hydrated with 10 mM HEPES buffer (pH 7.4), followed by heating in a water bath at 65 °C, and vortexing for 10 min. The heat and vortex cycle was repeated 10 times. The lipid suspension was sequentially extruded (Avanti Polar Lipids, Alabaster, AL, U.S.A.) through polycarbonate membranes of 200, 100, and 50 nm pore size. The extrusion was performed at 65°C and repeated 21 times for each pore size. The hydrodynamic diameter and ξ-potential of the liposomes were characterized using a Malvern Zetasizer Nano ZS (Worcestershire, U.K.). Measurement was conducted for each liposome solution (total lipid conc. of 1.0 and 2.0 mM for size and ξ-potential measurement, respectively) in 10 mM HEPES buffer (pH 7.4). In the case of the

liposome/HSA mixture, HSA was mixed with each liposome in 10 mM HEPES buffer (pH 7.4) and samples were incubated for 20 h before measurement.

3.2.6. Liposome stability in physiological saline.

10 μL of liposome solution (10 mM total lipid in 10 mM HEPES) was added to 90 μL of phosphate buffered saline (PBS) (pH 7.4). The mixture was incubated at room temperature for 20 h and then the particle size was measured. To investigate the stability in acidic aqueous solution, similar operation was carried out using PBS pH-controled with 0.1 M HCl*aq* (pH 2.6 and 4.0) instead of PBS (pH 7.4).

3.2.7. Liposome stability in physiological saline in the presence of HSA or other proteins.

10 μL of HSA (or ovalbumin or transferrin) solution with varying concentration (10 mM HEPES) was added to 10 μL of liposome solution (10 mM total lipid in 10 mM HEPES), and the resulting solution was incubated at room temperature for 30 min. The mixture was then diluted with 90 μL of PBS, and incubated at room temperature for 20 h, followed by particle size measurement.

3.2.8. Preparation of maleylated HSA (Mal-HSA).

Mal-HSA was prepared using a published method [10]. Briefly, 30 mg of HSA dissolved in 15 mL of $Na_2B_4O_7$ (pH 9.0) was reacted with excess solid maleic anhydride (46 mg) at ambient temperature. The pH was maintained at pH 8.5 by dropwise addition of 0.1 N NaOH. After 10 min of reaction, the product was purified on a PD-10 column (GE Healthcare) with ultra-pure water as eluent, and then lyophilized. The modification ratio of maleic acid to HSA was determined from the molecular weight of the resulting Mal-HSA measured using an Autoflex III

MALDI-TOF mass spectrometer (Bruker Daltonics, Bremen, Germany). MS (MALDI) *m/z*: found, 71579.9. Thus, 53 of the total 59 lysine residues in HSA were modified with maleic acid.

3.2.9. Binding of 8-anilino-1-naphthalenesulfonate (ANS) to HSA or Mal-HSA.

Titration of ANS binding to HSA or Mal-HSA was conducted using a published method [11]. Briefly, a stock solution of HSA or Mal-HSA (6.0 μM) in 10 mM HEPES (pH 7.4), and a stock solution of sodium 8-anilino-1-naphthalenesulfonate (Tokyo Chemical Industry) in 10 mM HEPES (pH 7.4) were mixed to prepare a series of solutions with varying ANS concentrations and constant HSA or Mal-HSA concentration (2.0 μM). Fluorescence resulting from ANS bound to HSA or Mal-HSA was measured using a spectrofluorometer FP8600 (Jasco corporation, Tokyo, Japan). The excitation and emission wavelengths were 372 and 466 nm, respectively.

3.2.10. Cell lines and cell culture.

Murine macrophage (RAW264.7) cells were cultivated in DMEM with 4.5 mg L-glutamine/L (10% fetal bovine serum (FBS) and antibiotics). The cells were maintained at 37°C/5% CO_2 in a humidified incubator.

3.2.11. Fluorescence microscopy.

Cells were seeded at a density of 2×10^4 cells per well in 96-well plates and cultured in DMEM containing 10% FBS overnight. Cells were incubated with DiO-labeled liposomes at concentrations of 1.0 mM total lipid and 0.1 mM HSA for 30 min in AIM-V serum free medium. Cells were then washed twice with PBS and AIM-V serum free medium was added. The uptake of liposomes by the cells was examined using a Biozero BZ-8100 fluorescence microscope (Keyence, Osaka, Japan).

3.2.12. Flow cytometry.

Cells were seeded at a density of 3×10^5 cells in 1.5 mL tubes. Cells were incubated with 220 μL of DiO-labeled liposome solution at concentrations of 2.7 mM total lipid and 270 μM HSA for 30 min in AIM-V serum free medium. 1 mL of PBS was added to the cells, which were then centrifuged at 1200 rpm for 5 min. The supernatant was replaced with 1 mL PBS. After additional centrifugation at 1200 rpm for 5 min, the supernatant was removed and cells were resuspended in 1 mL of PBS. Fluorescence data were collected using a Cell Analyzer EC800 (Sony, Tokyo, Japan).

3.3. Results and Discussions

3.3.1. Ligand structures facilitate binding with HSA.

I designed three ligand-modified lipids (**Scheme 3.1**). The ligands were modified at the amino-terminus of DSPE-PEG_{2k} via an amide bond. Decanoate (**1**) and stearate (**2**) are simple hydrophobic alkyl ligands, while octadecanedioate (**3**) has an ionizable carboxyl group at the terminus. First, I prepared liposomes from each ligand-modified lipid mixed with standard components (DSPC: cholesterol: ligand-modified lipid = 56: 39: 1) via the hydration method using 10 mM HEPES buffer as a solvent. The size of the liposomes was then adjusted by extrusion. As shown in **Figure 3.2A**, the liposomes containing **1** or **2** showed a narrow size distribution, while the liposomes containing **3** showed aggregation, probably due to hydrophobic interaction between the ligands. The "aggregation" may not be a simple aggregate but other structures such as multilamellar vesicles or two-dimensional lamellar structures. The stable nature of the liposome containing **2** is thought to be due to the insertion of stearate into the liposomal membrane to form a loop of PEG chain [1]. The reason for the difference in colloidal stability of the liposomes containing **1** compared with those containing **2**, is discussed later. The aggregation of the liposomes containing **3**, indicates that the ionizable octadecanedioate is exposed to the aqueous phase, which is appropriate for biding with HSA, however the aggregation must be minimized.

To suppress the aggregation of the liposome containing **3**, I examined the effect of mixing DSPE-PEG_{2k} into the bilayer to weaken the lateral and interparticle interactions among the ligands, through steric hindrance caused by PEG_{2k}. The total content of DSPE-PEG_{2k} and ligand-modified lipid was fixed at 5 mol%, which is understood to be the content of PEG_{2k} required to almost cover the liposome surface

with a mushroom conformation [12]. As shown in **Figure 3.2B**, aggregation was suppressed when the liposomes contained up to 2 mol% of **3**. The liposomes containing 2 mol% of **1** or **2** were also colloidally stable. Next, I examined the effect of addition of HSA (HSA/ligand ratio = 0.5) to the liposomes, on their size and ζ-potential (**Table 3.1**). Significant difference was only observed for the liposome containing **3**; for which slight decreases in size and polydispersity index were measured in the presence of HSA. These results indicate that a small population of aggregates was present, which were dissociated by coating with HSA.

Next, I examined the effect of physiological saline conditions (PBS) on the colloidal stability of the liposomes. As shown in **Figure 3.2C**, the liposomes containing **1** or **3** were aggregated in PBS. This is thought to be due to the enhanced hydrophobic interaction between the ligands under the high ionic strength conditions. It is notable that the liposomes containing **1** were not aggregated in 10 mM HEPES buffer (**Figure 3.2A**), showing that the decanoate of **1** tends to be exposed in the aqueous phase, but interparticle hydrophobic interaction is not sufficient to induce aggregation in 10 mM HEPES buffer. The liposome containing **2** was found to be stable in PBS, indicating the favorable nature of the anchoring of stearate into the liposomal membrane. When 100 μM of HSA was added, the aggregation of the liposomes containing **1** or **3** in PBS was suppressed (**Figure 3.2D**). This result clearly indicates that capping of the hydrophobic ligands with HSA suppresses the hydrophobic interaction between the ligands.

As previously described, the pockets of HSA have cationic amino acids at the bottom to bind with anionic carboxylates of fatty acids. It is therefore expected that **3** will interact more strongly with the pockets of HSA than **1**. In a comparable system, insulin modified with octadecanedioate was reported to have a stronger affinity for HSA than insulin modified with an alkyl group [13]. To establish the importance of the

hydrophobic pockets of HSA on the binding with the ligands of liposomes, I used maleylated HSA (Mal-HSA) [10], in which most of the cationic lysine residues (ca. 90%) were converted to anionic carboxylate by the reaction with maleic anhydride. I confirmed that Mal-HSA almost completely lost the ability to bind to an anionic dye, 8-anilinonaphthalene-1-sulfonic acid (ANS) (**Figure 3.3A**), indicating the successful modification of the hydrophobic pockets with cationic bottom in Mal-HSA. I found that Mal-HSA had no effect on the PBS tolerance of the liposomes containing **3** (**Figure 3.3B**). This result demonstrates the crucial role of the HSA hydrophobic pockets with cationic bottom on the binding with the octadecanedioate of **3**. The binding of HSA to the liposomes containing **3** was further confirmed by separating bound HSA on the liposomes by ultracentrifugation. Significant amount of HSA was precipitated by the liposomes containing **3**, while the precipitation HSA was negligible by the liposome without ligand (**Figure 3.4**). These results showed specific binding of HSA to the ligand on the liposome surface.

To further obtain proof that **3** is exposed to an aqueous solution, the size of liposome was monitored at acidic pH. At the neutral pH, the carboxyl group of **3** is usually in the state of carboxylate. On the other hand, the carboxylate will be protonated at acidic pH, and more hydrophobic **3** than deprotonated is predicted to be buried in liposome membrane, resulting in prevention of liposome aggregation. As expected, when the pH was decreased, the liposome containing **3** was suppressed to aggregate, indicating that exposed **3** was protonated and buried in liposome surface (**Figure 3.5**).

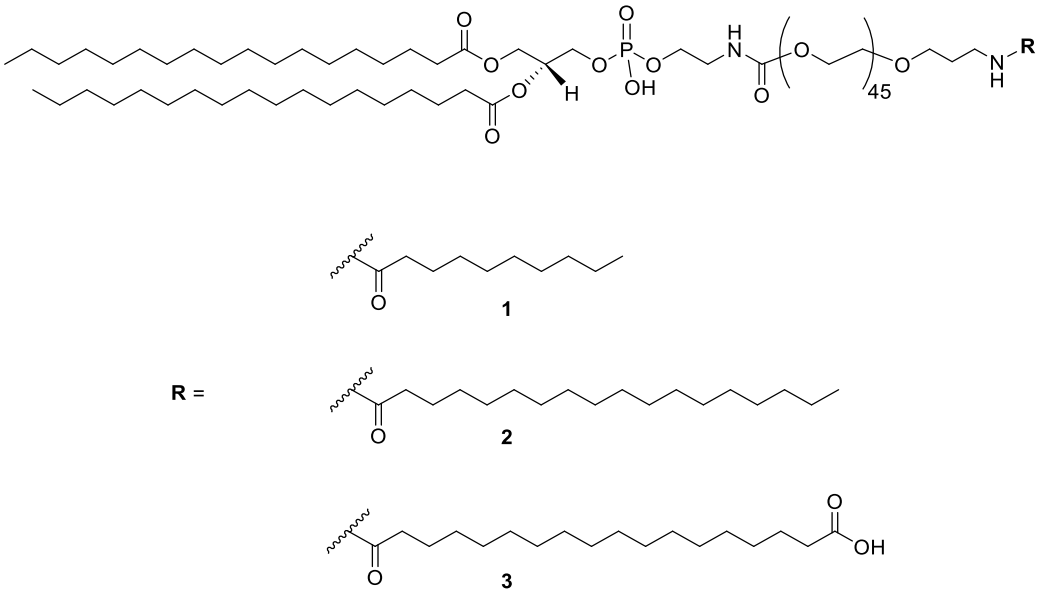

Scheme 3.1. Chemical structure of three kinds of ligand-modified lipids **1**-**3**. © 2018 American Chemical Society.

Table 3.1. Characteristics of liposomes in 10 mM HEPES (pH 7.4) in the presence or absence of HSA.

Liposome	Molar ratio	HSA[a]	Size (nm)	Polydispersity index	ζ-potential (mV)
DSPC/Chol/DSPE-PEG$_{2k}$/**1**	56/39/3/2	-	90	0.05	-20.2
		+	92	0.05	-25.6
DSPC/Chol/DSPE-PEG$_{2k}$/**2**	56/39/3/2	-	106	0.04	-19.9
		+	107	0.04	-21.1
DSPC/Chol/DSPE-PEG$_{2k}$/**3**	56/39/3/2	-	135	0.16	-21.3
		+	106	0.07	-22.9
DSPC/Chol/DSPE-PEG$_{2k}$	56/39/5	-	110	0.05	-15.6
		+	115	0.07	-14.6

[a] In the absence (-) or presence (+) of HSA (HSA/ligand mole ratio = 0.5). Chol: cholesterol.

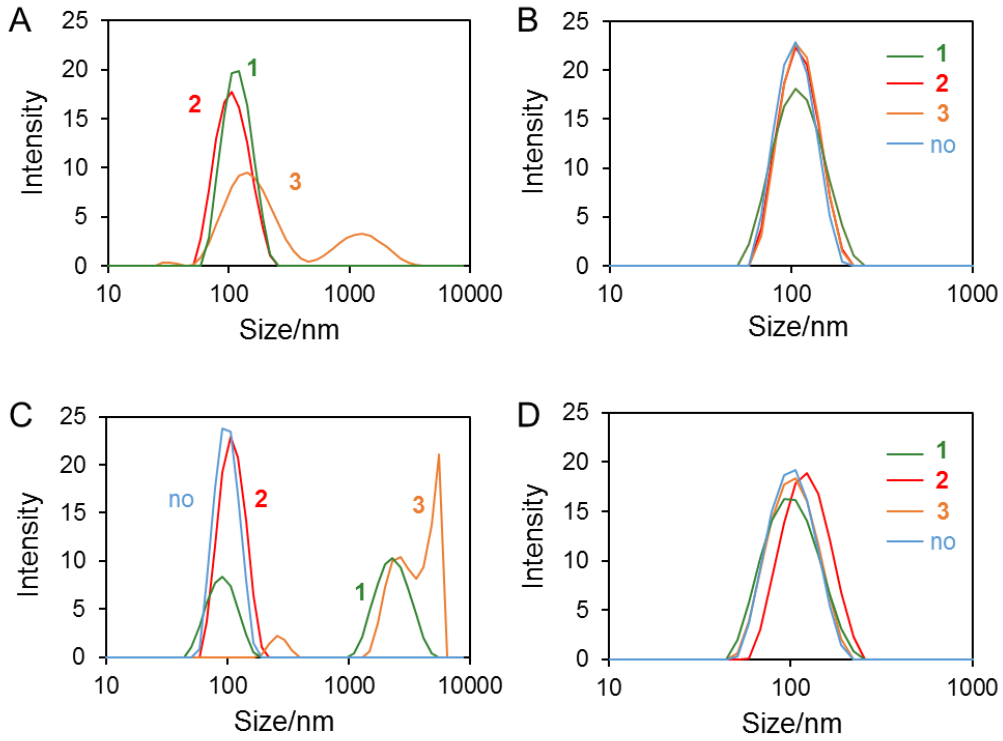

Figure 3.2. Size distributions of liposomes containing 1 mol% of ligand-modified lipid (**1**, **2** or **3**) in 10 mM HEPES (A). Size distribution of liposomes containing 2 mol% of ligand-modified lipid (**1**, **2** or **3**) and 3 mol% DSEP-PEG_{2k} in 10 mM HEPES (B), in PBS (C), and in PBS containing 100 μM HSA (D). "no" indicates liposomes containing 5 mol% DSEP-PEG_{2k} without a ligand-modified lipid component. Total lipid concentration of each liposome was 1.0 mM in all measurements. © 2018 American Chemical Society.

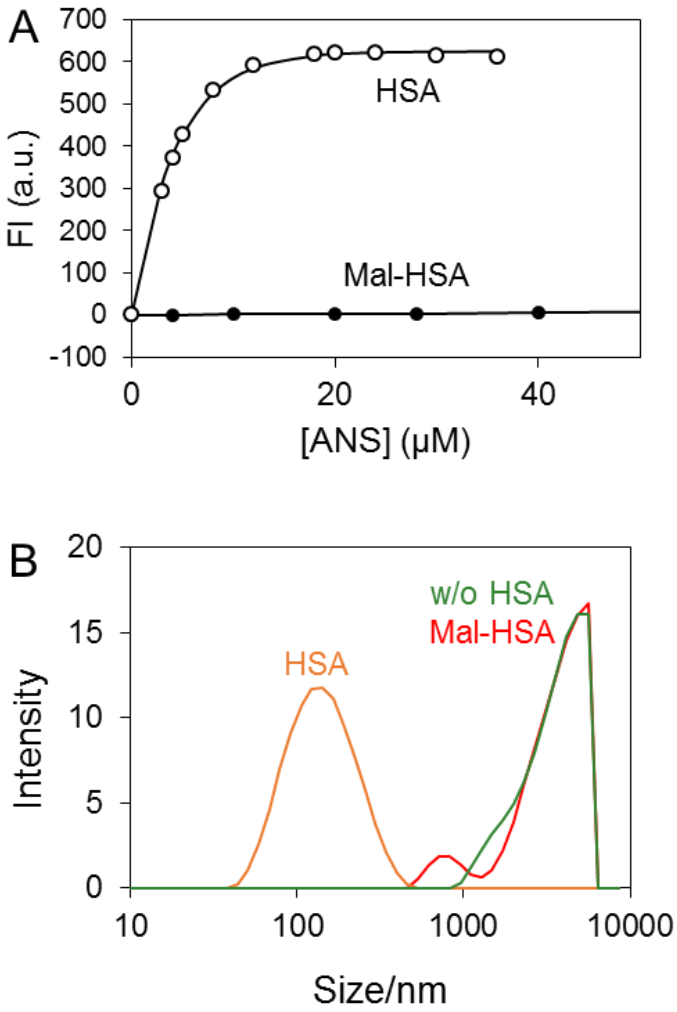

Figure 3.3. (A) Titration of HSA or Mal-HSA (2.0 μM) with ANS detected by fluorescence of ANS bound to HSA or Mal-HSA. ANS is a microenvironment-sensitive fluorescence probe which becomes strongly fluorescent once bound to the hydrophobic pockets of HSA [11]. (B) Size distribution of liposomes containing 2 mol% of ligand-modified lipid **3** and 3 mol% of DSEP-PEG_{2k} in PBS or in PBS containing HSA or Mal-HSA (100 μM). Total lipid concentration of liposomes was 1.0 mM.

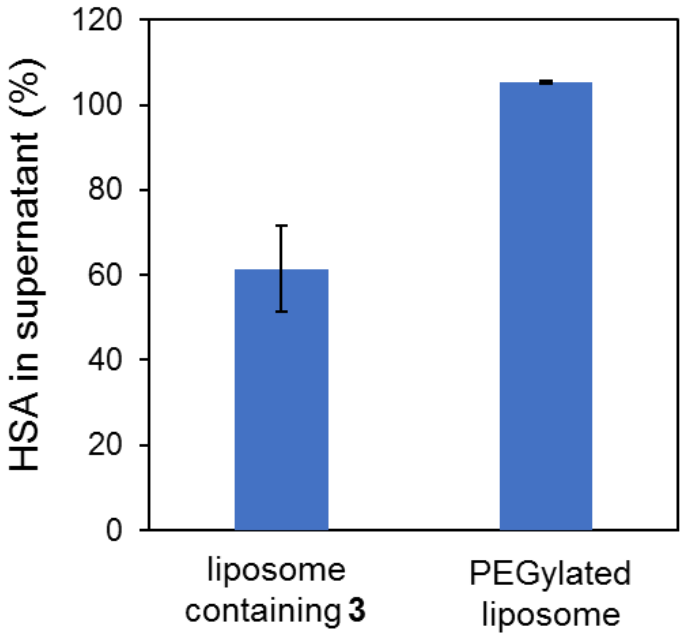

Figure 3.4. The fluorescence intensity of rhodamine-labeled HSA in supernatant after ultracentrifugation of mixture of liposomes and rhodamine-labeled HSA. 10 μL of solution of liposome containing **3** or PEGylated liposome (100 nmol total lipid in 10 mM HEPES) was mixed with 100 μL of rhodamine-labeled HSA (1 nmol in HEPES). Mole ratio of HSA/**3** was 0.5. Then, the mixture was incubated for 30 min at room temperature for the complex formation. To the mixture, 890 μL of PBS was added and the resulting solution was centrifuged at 200,000 × g for 30 min to separate liposome/HSA complex from free HSA. The amount of rhodamine-labeled HSA in the supernatant was quantitated by fluorescence intensity measurement (em. 530 nm, ex. 590 nm).

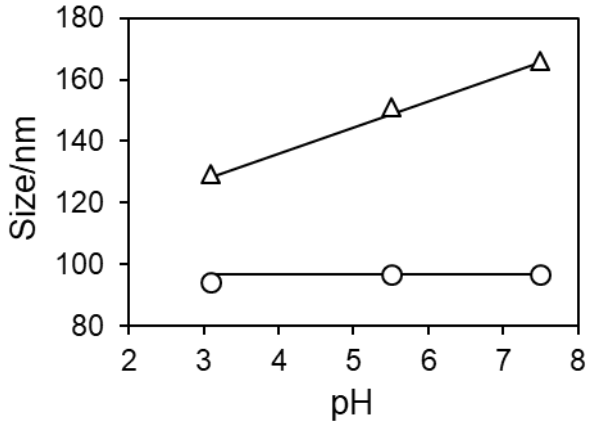

Figure 3.5. Liposome average size in PBS at different pH. © 2018 American Chemical Society.

3.3.2. Stoichiometry of ligand binding with HSA.

The minimum amount of HSA required to suppress the aggregation of liposomes containing **3** was examined to estimate the stoichiometry of binding between the ligand (octadecanedioate) and HSA. Thus, liposomes containing varying molar ratios of **3** were prepared with constant total content of DSPE-PEG_{2k} and **3** (5 mol%). As shown in **Figure 3.6**, at lower HSA/**3** mole ratios (< 10^{-3}), the liposomes were aggregated and the size of the aggregates became smaller with decreasing **3** content, indicating that the aggregation of the liposomes was induced by interparticle interaction between the ligands. The liposome with the lowest content of **3** (0.1 mol%) showed no detectable aggregation. The size of the aggregates of each liposome abruptly decreased within a narrow HSA/**3** ratio range and became equal to liposome size (~100 nm) at the HSA/**3** ratio of 10^{-1}. Because half of the ligand molecules are in the outer leaflet of the bilayer, making them available for effective binding with HSA (the other half of the ligand molecules are in the inner leaflet), an HSA/**3** ratio of ~1/5 is sufficient to prevent the interparticle aggregation of the liposomes. The requirement of only a small amount of HSA for stabilization of the liposomes may be explained by the use of multiple HSA pockets for ligand binding. **Figure 3.7** shows three possible orientations of HSA toward the liposome surface to achieve binding to as many ligands as possible. The underlined numbers indicate the pockets whose entrance for accommodation of the ligand faces the surface of the liposome, making it capable of binding with the ligand. These three orientations enable HSA to bind with four or five ligands. In the face-on orientation in particular, all of the strong binding pockets, 2, 4 and 5 [4], face the liposome surface.

Figure 3.8 shows the expected structure of the face-on binding of HSA to the liposome surface. It was reported that conformational transition of PEG chains from mushroom to brush begins to take place at 5 mol% DSPE-PEG_{2k} [12]. The present

liposome surface is therefore almost completely covered with PEG_{2k} in a mushroom conformation. The diameter of PEG_{2k} with a mushroom conformation is given by the Flory radius (3.5 nm) [14] and thus the projection area of PEG_{2k} is calculated to be 9.6 nm^2. In **Figure 3.8**, the PEG_{2k} components of **3** and DSPE-PEG_{2k} are shown in pink and blue, respectively. Five ligands are expected to bind to one HSA through five pockets, shown in **Figure 3.8B**. Since the surface area occupied by one HSA molecule is calculated to be 70 nm^2 (longest and shortest axes are 8.7 and 8.1 nm, respectively), the surface coverage of liposomes with HSA was calculated to be 53% for the liposomes containing 2 mol% of **3**.

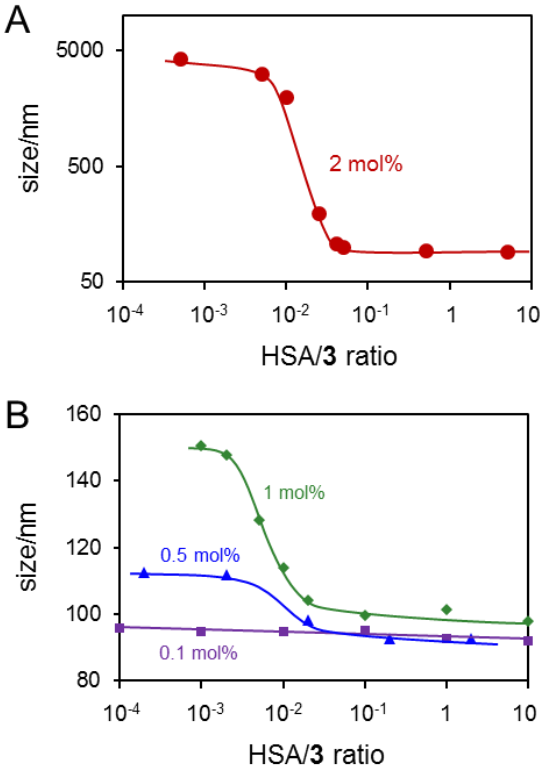

Figure 3.6. Determination of critical mixing ratio HSA/**3** to suppress interparticle aggregation of liposomes. Four kinds of liposomes with varying **3** content (0.1, 0.5, 1, and 2 mol%) with constant total content of **3** and DSEP-PEG_{2k} (5 mol%) were mixed with HSA in PBS. Total lipid concentration of each liposome was 1.0 mM in all measurements.

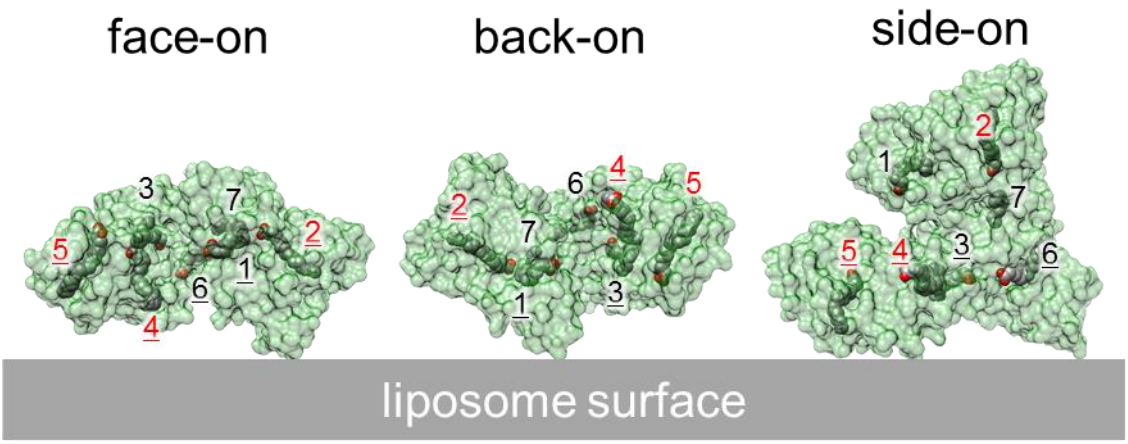

Figure 3.7. Three possible orientations of HSA binding to the liposome surface. Underlined site numbers have potential to bind with an octadecanedioate ligand because the entrance to these sites directs toward the liposome surface. Site numbers shown in red are strong binding sites. © 2018 American Chemical Society.

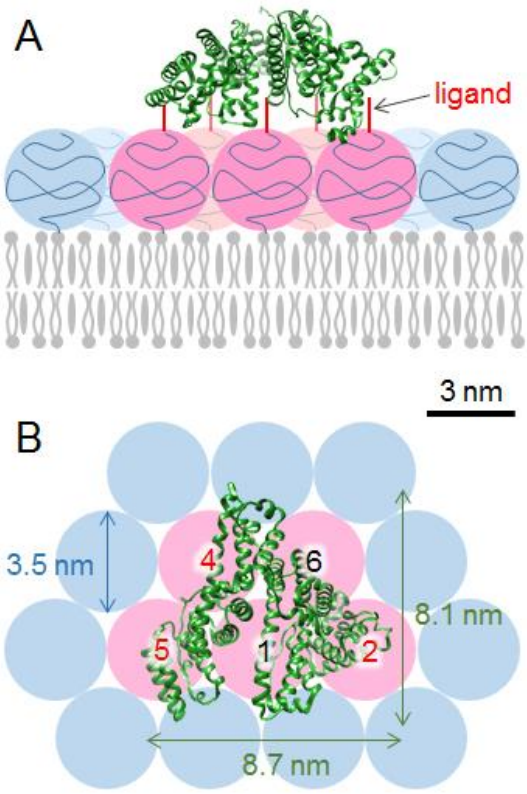

Figure 3.8. Schematic representation of HSA bound to five ligands (octadecanedioate) via each pocket (1, 2, 4, 5 and 6) in face-on orientation. Side view (A) and top view (B). © 2018 American Chemical Society.

3.3.3. Specificity of ligand binding to HSA.

To establish the specificity of binding of the ligand to HSA, I examined binding behavior of other proteins that have similar molecular weight and pI to HSA, but have no fatty acid binding sites to the ligand modified liposomes. Ovalbumin (45 kDa, pI 4.5) and transferrin (77 kDa, pI 5.9) were chosen for this purpose. As shown in **Figure 3.9**, these two proteins also suppressed the interparticle aggregation of the liposomes, however they were required at more than one hundred times higher concentration than HSA. This supports the findings that octadecanedioate ligands presented on the liposome surface bind specifically with the hydrophobic pockets of HSA.

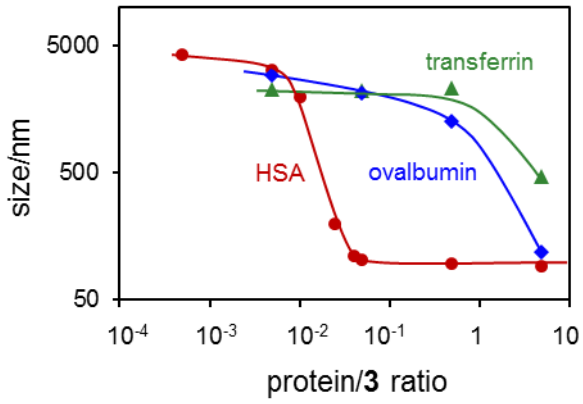

Figure 3.9. Selectivity of interaction of liposomes containing 2 mol% of **3** and 3 mol% of DSPE-PEG_{2k} with three proteins of similar size and pI. Total lipid concentration of each liposome was 1.0 mM. © 2018 American Chemical Society.

3.3.4. Macrophage recognition of HSA-coated liposomes.

Finally, I examined phagocytotic uptake of the HSA-coated liposomes by macrophage Raw264.7. The liposomes containing 2 mol% of **3** and 3 mol% of DSPE-PEG_{2k} were coated with HSA (HSA/**3** mole ratio: 5) and applied to Raw264.7 cells in serum free medium. Phagocytotic uptake of the HSA-coated liposomes is almost the same as that of 5 mol% PEGylated liposomes, which are inert to recognition by macrophages (**Figure 3.10A, B**) [15]. The inertness of the HSA-coated liposome is thought to be due to the high PEG density consisted of **3** and DSPE-PEG_{2k}. **Figure 3.11A** shows the phagocytotic uptake of 3-mol% PEGylated liposome without the ligand modified lipid (DSPC: cholesterol: DSPE-PEG_{2k} = 56:39:3), and it was higher than that of 5-mol% PEGylated one. The enhanced cellular uptake of 3-mol% PEGylated liposome will be due to the incomplete surface coating of this liposome. On the other hand, when the liposome containing 2 mol% of **3** and 3 mol% of DSPE-PEG_{2k} were in the medium without HSA, more active uptake by macrophages was observed (**Figure 3.11B**). The inertness of the HSA-coated liposomes contrasts sharply with that for liposomes covalently modified with BSA, which were taken up relatively efficiently by macrophages [15]. In that case, authors used BSA whose lysine residues were converted to neutral thioacetate, which makes the net charge of BSA more anionic for recognition by scavenger receptors, which nonspecifically recognize anionic proteins. Thus, I can conclude that HSA-coated liposomes prepared using our method are inert in scavenger receptor-mediated phagocytosis by macrophages. I compared the inertness of our liposome with liposomes coated with HSA by physical adsorption, which were prepared following a literature [16,17]. As a result, the physically coated liposomes were more actively taken up by macrophages (**Figure 3.11C**). This will be due to the instability of physically adsorbed HSA layer on the liposome surface. The instability of the physically adsorbed HSA layer was confirmed

by the tolerance of the liposomes against solutions containing physiological saline or fetal bovine serum (**Figure 3.12**).

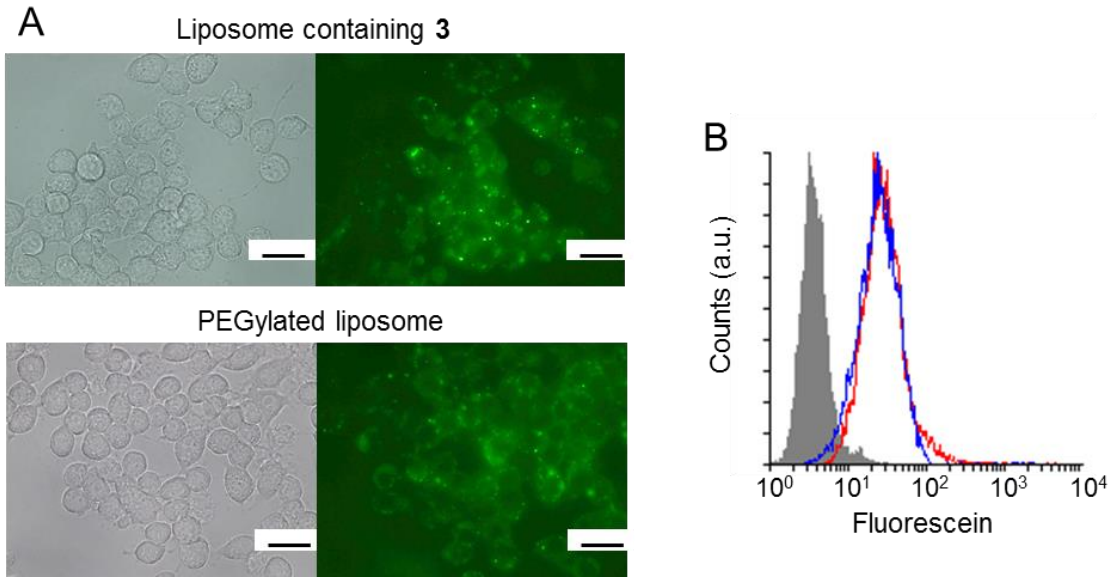

Figure 3.10. Uptake of DiO-labeled liposomes by Raw264.7 macrophages observed using fluorescence microscopy (A) and by flow cytometry (B). In A, liposomes containing 2 mol% of **3** and 3 mol% of DSPE-PEG_{2k} (upper panel) and those containing 5 mol% DSPE-PEG_{2k} (lower panel). Scale bars: 20 μm. In B, blue and red lines show liposomes containing 2 mol% of **3** and 3 mol% of DSPE-PEG_{2k} and those containing 5 mol% DSPE-PEG_{2k}, respectively. Shaded area indicates non-treated Raw264.7. Mole ratio of HSA/**3** was 5 in the both experiments. © 2018 American Chemical Society.

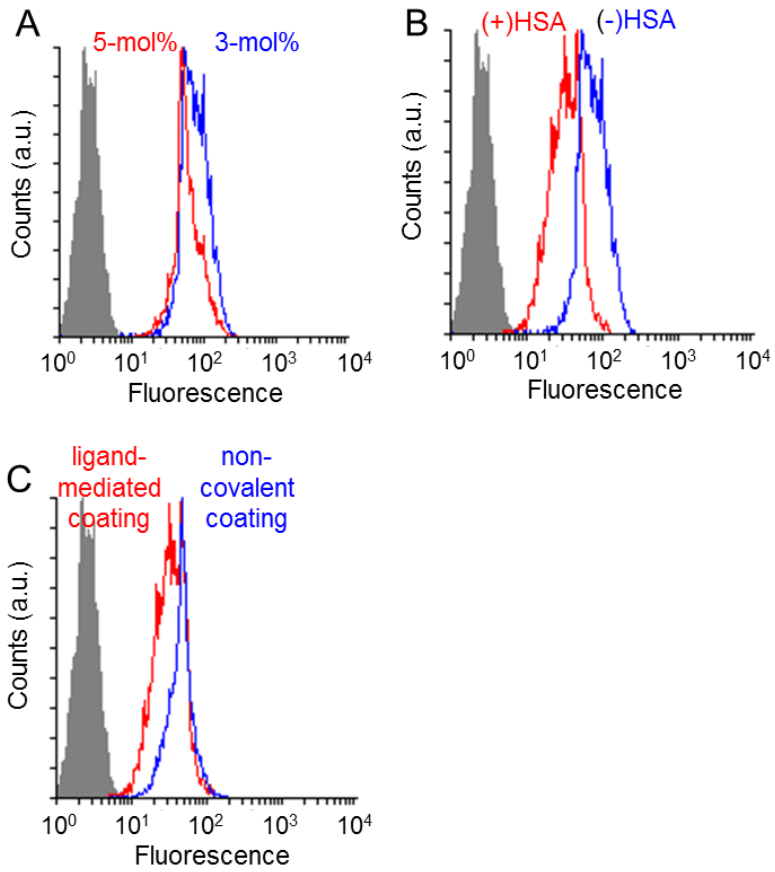

Figure 3.11. Uptake of DiO-labeled liposomes by Raw264.7 macrophages observed by flow cytometry (ex. 488 nm; em. 525/50 nm). (A) Comparison between 3- and 5-mol% PEGylated liposomes. (B) Comparison of liposomes (2 mol% of **3** and 3 mol% of DSPE-PEG_{2k}) in the presence and absence of HSA (HSA/**3** = 5). (C) Comparison of liposomes (2 mol% of **3** and 3 mol% of DSPE-PEG_{2k}) coated with HSA via ligand and liposomes (DPPC: cholesterol = 7:3) coated with HSA by physical adsorption. For the physical adsorption coating, I followed a reported procedure [17]. Briefly, 10 μL of liposome solution (10 mM total lipids in PBS) and 10 μL of HSA solution (1 mM in 10 mM HEPES) were mixed and incubated for 1 hour at 37℃ (HSA/**3** = 5). The experimental procedures for cellular uptake and flow cytometry were same with **Figure 3.10**. In A-C, shaded area indicates non-treated Raw264.7. © 2018 American Chemical Society.

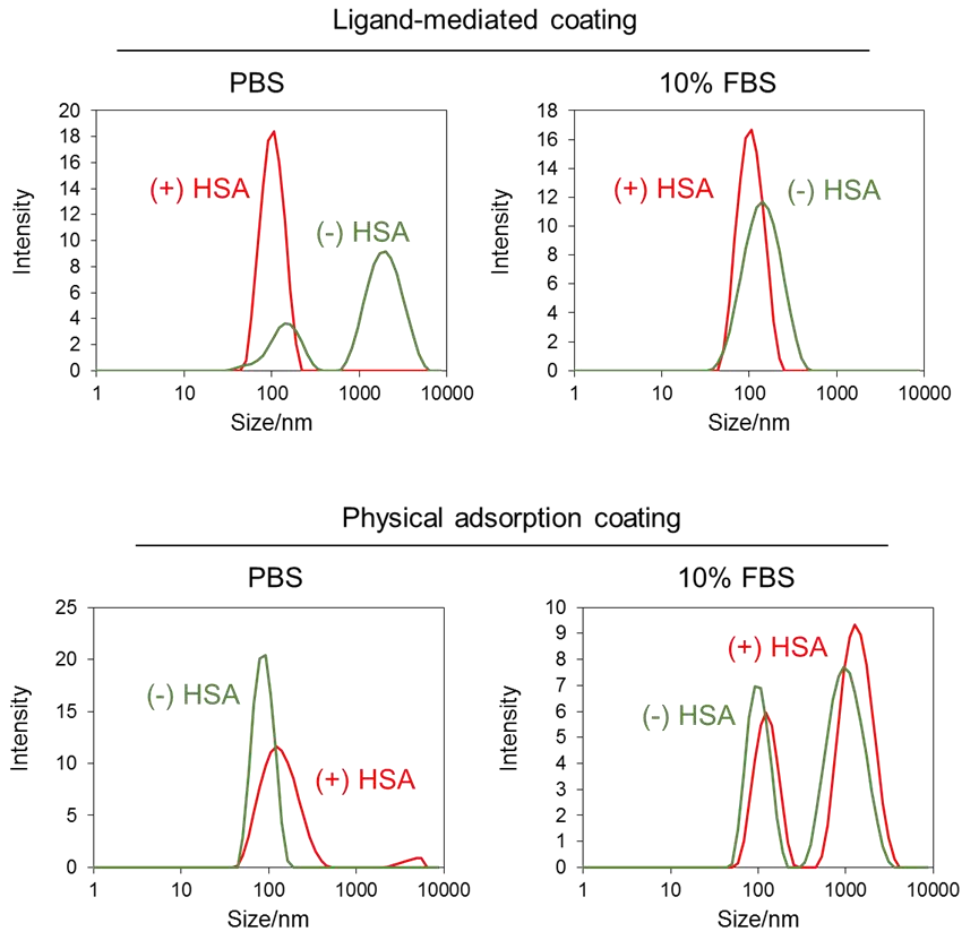

Figure 3.12. Size distributions of two kinds of liposomes after 3 hours from dilution with two kinds of solvents (PBS or 10% FBS-containing medium) in the presence or absence of HSA. Liposomes (2 mol% of **3** and 3 mol% of DSPE-PEG_{2k}) coated with HSA via ligand and liposomes (DPPC: chol = 7:3) coated with HSA by physical adsorption were used. 10 μL of each liposome solution (10 mM total lipids in 10 mM HEPES) and 10 μL of HSA solution (1 mM in 10 mM HEPES) were mixed, and incubated at 37℃ for 1 h for surface coating. Then, the mixture was diluted with 80 μL of PBS or culture medium (AIM-V) containing 10% fetal bovine serum (FBS), and the resulting solution was incubated at 37℃ for 3 hours. © 2018 American Chemical Society.

3.4. Conclusions

Here I proposed for the first time the coating of liposome surfaces with HSA via specific hydrophobic ligands. I found that a short alkyl (decanoate) or long alkyl with carboxyl terminus (octadecanedioate) could avoid burial into the liposomal membrane and facilitate binding with HSA. The binding of ligand-modified liposomes is considerably more specific to HSA than to other proteins (transferrin and ovalbumin). The HSA-coated liposomes are as inert as PEGylated liposomes to phagocytotic uptake by macrophages. All of the previous reports of HSA (or BSA)-coated liposomes are prepared using covalent bonds. Compared with these covalent methods, our non-covalent coating is advantageous because the coating can be applied at the time of use by mixing with fresh HSA. Our HSA-coated liposomes could be useful as drug carriers with improved colloidal stability in blood. HSA is known to accumulate in tumor through gp60 expressing on endothelial cells [18]. HSA-coated nanoparticles have been speculated to accumulate in tumor via this pathway [19]. Thus, our HSA-coated liposome may be useful for tumor targeting.

3.5. References

[1] Hansen, M. B.; van Gaal, E.; Minten, I.; Storm, G.; van Hest, J. C. M.; Löwik, D. W. P. M. Constrained and UV-activatable cell-penetrating peptides for intracellular delivery of liposomes. *J. Control. Release* **2012**, *164*, 87-94.

[2] Bhattacharya, A. A.; Grüne, T.; Curry, S. Crystallographic analysis reveals common modes of binding of medium and long-chain fatty acids to human serum albumin. *J. Mol. Biol.* **2000**, *303*, 721-732.

[3] Simard, J. R.; Zunszain, P. A.; Hamilton, J. A.; Curry, S. Location of high and low affinity fatty acid binding sites on human serum albumin revealed by NMR drug-competition analysis. *J. Mol. Biol.* **2006**, *361*, 336-351.

[4] Simard, J. R.; Zunszain, P. A.; Ha, C.-E.; Yang, J. S.; Bhagavan, N. V.; Petitpas, I.; Curry, S.; Hamilton, J. A. Locating high-affinity fatty acid-binding sites on albumin by x-ray crystallography and NMR spectroscopy. *Proc. Natl. Acad. Sci. USA* **2005**, *102*, 17958-17963.

[5] Richieri, G. V.; Anel, A.; Kleinfeld, A. M. Interactions of long-chain fatty acids and albumin: Determination of free fatty acid levels using the fluorescent probe ADIFAB. *Biochemistry* **1993**, *32*, 7574-7580.

[6] Eberhart, R. C.; Munro, M. S.; Williams, G. B.; Kulkarni, P. V.; Shannon, W. A. Jr.; Brink, B. E.; Fry, W. J. Albumin adsorption and retention on C_{18}-alkyl-derivatized polyurethane vascular grafts. *Artif. Organs.* **1987**, *11*, 375-382.

[7] Pitt, W. G.; Cooper, S. L. Albumin adsorption on alkyl chain derivatized polyurethanes: I. The effect of C-18 alkylation. *J. Biomed. Mater. Res.* **1988**, *22*, 359-382.

[8] Pitt, W. G.; Grasel, T. G.; Cooper, S. L. Albumin adsorption on alkyl chain derivatized polyurethanes. II. The effect of alkyl chain length. *Biomaterials* **1988**, *9*, 36-46.

[9] Wang, D.; Ji, J.; Gao, C.; Yu, G.; Feng, L. Surface coating of stearyl poly(ethylene oxide) coupling-polymer on polyurethane guiding catheters with poly(ether urethane) film-building additive for biomedical applications. *Biomaterials* **2001**, *22*, 1549-1562.

[10] Alford, P. B.; Xue, Y.; Thai, S. -F.; Shackelford, R. E. Maleylated-BSA enhances production of nitric oxide from macrophages. *Biochem. Biophys. Res. Commun.* **1998**, *245*, 185-189.

[11] Takehara, K.; Yuki, K.; Shirasawa, M.; Yamasaki, S.; Yamada, S. Binding properties of hydrophobic molecules to human serum albumin studied by fluorescence titration. *Anal. Sci.* **2009**, *25*, 115-120.

[12] Garbuzenko, O.; Barenholz, Y.; Priev, A. Effect of grafted PEG on liposome size and on compressibility and packing of lipid bilayer. *Chem. Phys. Lipids* **2005**, *135*, 117-129.

[13] Jonassen, Ib; Havelund, S.; Hoeg-Jensen, T.; Steensgaard, D. B.; Wahlund, P.; Ribel, U. Design of the novel protraction mechanism of insulin degludec, an ultra-long-acting basal insulin. *Pharm. Res.* **2012**, *29*, 2104-2114.

[14] deGennes, P. G. Conformations of polymers attached to an interface. *Macromolecules* **1980**, *13*, 1069-1075.

[15] Vuarchey, C.; Kumar, S.; Schwendener, R. Albumin coated liposomes: a novel platform for macrophage specific drug delivery. *Nanotechnol. Devel.* **2011**, *1*, e2.

[16] Yoshida, A.; Hashizaki, K.; Yamauchi, H.; Sakai, H.; Yokoyama, S.; Abe, M. Effect of lipid with covalently attached poly(ethylene glycol) on the surface properties of liposomal bilayer membranes. *Langmuir* **1999**, *15*, 2333-2337.

[17] Yokouchi, Y.; Tsunoda, T.; Imura, T.; Yamauchi, H.; Yokoyama, S.; Sakai, H.; Abe, M. Effect of adsorption of bovine serum albumin on liposomal membrane characteristics. *Colloids Surf., B* **2001**, *20*, 95-103.

[18] Tiruppathi, C.; Song, W.; Bergenfeldt, M.; Sass, P.; Malik, A. B. Gp60 activation mediates albumin transcytosis in endothelial cells by tyrosine kinase-dependent pathway. *J. Biol. Chem.* **1997**, *272*, 25968-25975.

[19] Larsen, M. T.; Kuhlmann, M.; Hvam, M. L.; Howard, K. A. Albumin-based drug delivery: Harnessing nature to cure disease. *Mol. Cell. Ther.* **2016**, 4:3.

CHAPTER 4

Fc-III peptide-Mediated Coating of Liposome with Immunoglobulin G

4.1. Introduction

Liposome is the representative drug carrier that accommodates drugs inside and lipid bilayer. The long blood half-life of the liposome is crucial to efficient delivery to the target tissues. To improve the blood half-life, polyetheleneglycol (PEG)-grafting on the liposome surface is usually utilized [1]. However, antibodies against PEG are produced in human body which reduces the blood half-life of PEG-coated liposome [2,3].

In search for alternative coating molecules to prolong the blood half-life of the liposome, here I focused on immunoglobulin G (IgG). IgG is the second most abundant protein in blood, ~15 mg/mL (~100 μM), and has a quite long blood half-life of 7-21 days [4]. Some kinds of bacteria are known to avoid immunity by coating their surface with endogenous IgG through constant region [5]. Such constant region-mediated coating enables to utilize any IgGs independent of their valuable region. By learning from the bacteria, here I propose coating of liposome with IgG through constant region as shown in **Figure 4.1A**. I utilized a ligand to constant region to coat the surface of liposome via non-covalent way.

Several ligand proteins and peptides to constant region of IgG have been reported so far [6-9]. The bacteria utilize protein A and protein G to coat their surface [10,11]. Here I utilized a short peptide ligand, Fc-III peptide which binds to boundary of C_H2 and C_H3 region with relatively strong affinity (K_d = 25 nM) [12]. I modified

palmityol group on N-terminus of Fc-III peptide through hexaethylene glycol linker (**1**) (**Figure 4.1B**). Palmitoyl group functions as an anchor to liposomal membrane.

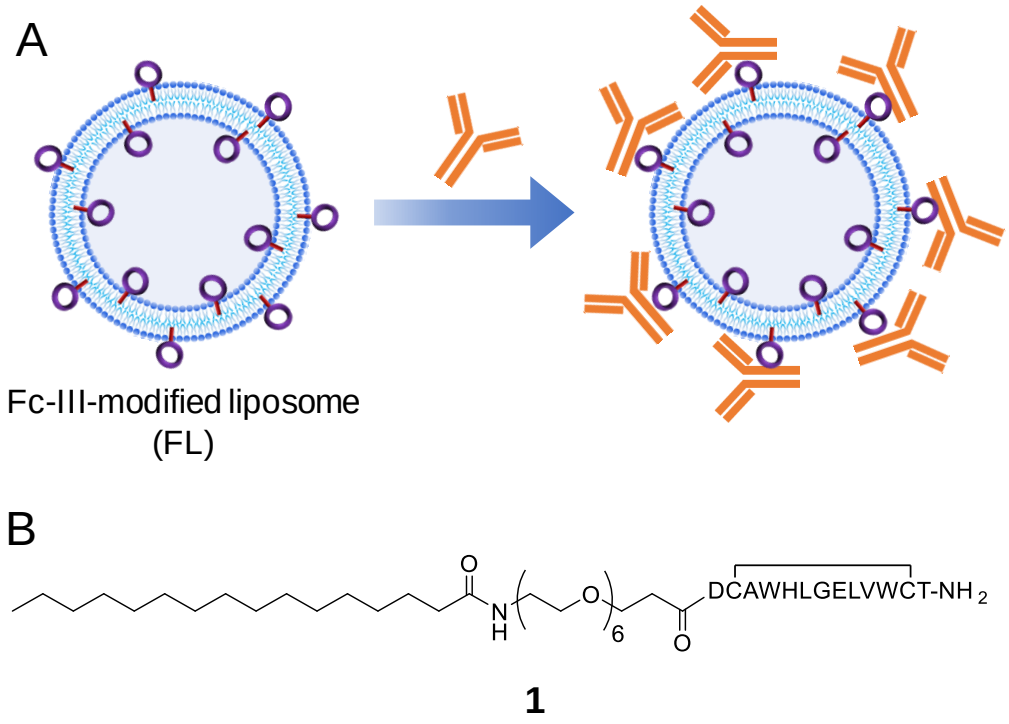

Figure 4.1. (A) Schematic illustration of coating of liposome surface with IgG via Fc-III peptide. (B) Chemical structure of palmytoylated Fc-III peptide (**1**).

4.2. Materials and Methods

4.2.1. Materials.

Rink Amide AM resin (200-400 mesh, amine density of 0.61 mmol g^{-1}) and all Fmoc-protected amino acids were purchased from Novabiochem (Darmstadt, Germany). Fmoc-NH-$(PEG)_5$-COOH was purchased from Merch Millipore (Burlington, NJ, U.S.A). Diisopropylethylamine (DIEA) and COMU were purchased from Watanabe Chemical Industry (Hiroshima, Japan). 1,2-Distearoyl-sn-glycero-3-phosphocholine (DSPC) were purchased from NOF corporation (Tokyo, Japan). Anti-CD20 mAb Ofatumumab (Arzerra) was purchased from Novartis (Basel, Switzerland). NHS-fluorescein and NHS-rhodamine were purchased from Thermo Fischer Scientific (Waltham, MA, U.S.A.). Palmitic acid was purchased from Tokyo Chemical Industry (Tokyo, Japan). RPMI-1640 was purchased from Nacalai Tesque (Kyoto, Japan).

4.2.2. Synthesis of palmitoylated Fc-III peptide (**1**).

N-terminally palmitoylated Fc-III peptide **1** was chemically synthesized by Fmoc solid phase peptide synthesis method using the Rink Amide AM resin, DIEA as a base, COMU as coupling reagents, and a 20% solution of piperidine in DMF for deprotection of Fmoc group. After the coupling reaction, to cleave peptide from resin, the resin was incubated with TFA/thioanisole/ultra-pure water/phenol/ethanedithiol (80:5:5:7.5:2.5 by volume) as cleavage cocktail at room temperature for 1.5 hours at RT. Then, the peptide was cyclized following a literature [13,14]. Briefly, the crude peptide was dissolved in 600 µL of DMSO containing 2 µL DIEA at RT for 21 h. The cyclized crude peptide was purified by standard reversed phase HPLC using C18 column (Waters, Tokyo, Japan). The obtained compound was identified by MALDI-TOF MS. MS m/z: calculated for $C_{100}H_{155}N_{19}NaO_{26}S_2$ ($M + Na^+$), 2126.1; found, 2125.7 (**Figure 4.2**).

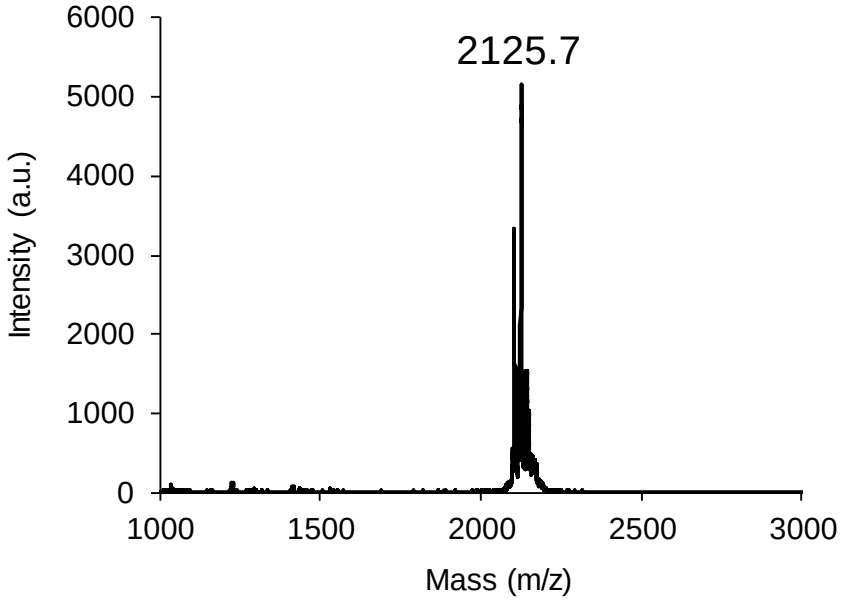

Figure 4.2. Identification of **1**. Calculated exact mass of **1**·Na^+ was 2125.1.

4.2.3. Preparation of liposomes.

Lipid hydration method was used for the preparation of liposomes. DSPC, cholesterol and **1** (60:39:1 mol%) were dissolved in a mixture of chloroform in a round bottom flask. To fluorescently label the liposome, 1 mol% of DiO was mixed with the lipids. The solvent mixture was evaporated at 65℃ to form a thin film of lipid mixture. Any trace of organic solvents was removed by keeping the film under vacuum for at least 2 h. The lipid film was hydrated with 10 mM HEPES buffer (pH 7.4) or PBS, followed by heating in a water bath at 65℃, and vortexing for 10 min. The heat and vortex cycle was repeated 10 times. The lipid suspension was sequentially extruded (Avanti Polar Lipids, Alabaster, AL, U.S.A.) through polycarbonate membranes of 200, 100, and 50 nm pore size. The extrusion was performed at 65℃ and repeated at 21 times for each pore size. The 150 μL of liposome suspension was diluted with 10 mM HEPES buffer (pH 7.4) to measure the particle size or ζ-potential by a Malvern Zetasizer Nano ZS instrument (Worcestershire, U.K.).

4.2.4. Liposome stability in physiological saline in the presence of IgG.

10 μL of anti-CD20 mAb solution with varying concentration (10 mM HEPES) was added to 10 μL of liposome solution (1.0 or 10 mM of total lipids in 10 mM HEPES), and the resulting solution was then diluted with 80 μL of 10 mM HEPES. After 30 min of incubation at room temperature, the particle size was measured by a Malvern Zetasizer Nano ZS instrument (Worcestershire, U.K.).

4.2.5. Rhodamine labeling of anti-CD20 mAb.

Anti-CD20 mAb was labeled with NHS-rhodamine according to manufacturer's protocols. 70 μL of dehydrated DMSO containing NHS-rhodamine (10 mg/mL) was added to 500 μL of Arzerra (20 mg/mL). After 2 h of reaction in the dark at 4℃, the

product was purified on a PD-10 columun (GE Healthcare, Amersham, U.K.) with PBS. The fluorophore to protein labeling ratio was 2.5 mol of dye per mole of mAb.

4.2.6. Fluorescein labeling of monoclonal IgG with high affinity to FcγRs

A monoclonal IgG with high affinity to FcγRs (mogamulizumab) was labeled with NHS-fluorescein according to manufacturer's protocols. 6.4 μL of dehydrated DMSO containing NHS-fluorescein (10 mg/mL) was added to 250 μL of Poteligeo (4 mg/mL). After 2 h of reaction in the dark at 4℃, the product was purified on a PD-10 columun (GE Healthcare, Amersham, U.K.) with PBS. The fluorophore to protein labeling ratio was 1.2 mol of dye per mole of mAb.

4.2.7. Fluorescence correlation spectroscopy (FCS).

The binding of rhodamine-labeled anti-CD20 mAbs to Fc-III-modified liposomes was determined by FCS. Measurements were performed with a confocal laser scanning microscope FV1000-D (Olympus, Tokyo, Japan) equipped with a 559 nm laser as an excitation light source and a 60× water immersion objective with a numerical aperture of 1.2 (UPLSAPO 60XW, Olympus, Tokyo, Japan) in the FCS mode. Samples of rhodamine-labeled CD20 mAb (1 μM) with FL or BL (total lipid: 10 mM), or without liposome were measured at room temperature on a μ-slide $VI^{0.4}$, IbiTreat (Ibidi, Planegg, Germany). The scan speed was 2 μs/pixel and scanning time was 32766 times. The obtained single data were divided into 63 sections and the datasets were analyzed by the equipped software. The diffusion time τ_D in the lateral detection area was obtained with calculated D as follows (equation 1).

$$\tau_D = \frac{\omega_0^2}{4D} \quad (1)$$

ω_0 is the lateral radius of detection area (0.222419 μm). The hydrodynamic radius r was calculated by Stokes-Einstein equation as follows:

$$\mathrm{D} = \frac{k_B T}{6\pi\eta r} \tag{2}$$

where k_B is the Boltzmann constant, T is the absolute temperature, η is the viscosity of the solvent, and r is the hydrodynamic radius.

4.2.8. Cell lines and cell culture.

JY25 cells, a lymphoblastoid human B cell line, and U937 cells, a human monocytic cell line, were cultivated in RPMI 1640 with L-glutamine (10% fetal bovine serum and antibiotics). The cells were maintained at 37℃/5% CO_2 in a humidified incubator.

4.2.9. Expression analysis of CD20 and FcγRs by flow cytometry.

Cells were seeded at a density of 6×10^5 cells in 1.5 mL tubes. After addition of 155 μL of fluorescence-labeled antibody solutions containing 234 μM rhodamine-labeled anti-CD20 IgG (ofatumumab) or 322 μM fluorescein-labeled monoclonal IgG of mogamulizumab which has high binding affinity to FcγRs the cells were incubated in RPMI-1640 culture medium for 30 min at 4℃. After washing twice with PBS, the cells were resuspended in 600 μL of PBS. Fluorescence data were collected using a Cell Analyzer EC800 (Sony, Tokyo, Japan).

4.2.10. Flow cytometry.

Cells were seeded at a density of 6×10^5 cells in 1.5 mL tubes. Cells were incubated with 300 μL of DiO-labeled liposome solution at concentrations of 0.25 mM total lipid and 1.3 μM anti-CD20 mAb in RPMI-1640 culture medium for 30 min at 4℃. After washing twice with PBS, the cells were resuspended in 600 μL of PBS. Fluorescence data were collected using a Cell Analyzer EC800 (Sony, Tokyo, Japan).

4.2.11. Fluorescence microscopy.

Cells were seeded at a density of 4×10^4 cells in 1.5 mL tubes. Cells were incubated with DiO-labeled liposomes at concentrations of 0.45 mM total lipid and 2.4 μM HSA in RPMI-1640 culture for 2 hours at 37℃. After washing twice with PBS, the cells were resuspended in 100 μL of PBS. The uptake of liposomes by the cells was examined using a Biozero BZ-8100 fluorescence microscope (Keyence, Osaka, Japan).

4.3. Results and Discussions

4.3.1. Characterization of prepared liposomes.

I designed Fc-III peptide modified with palmitate through hexaethylene glycol linker. The liposome was prepared by standard hydration technique by mixing 1 mol% of **1**. The liposome including **1** was successfully prepared with somewhat larger size than the liposome free of **1** (**Table 4.1**).

Table 4.1. Characteristics of liposomes in 10 mM HEPES (pH 7.4) in the presence and absence of IgG.

Liposome	Molar ratio	IgG[a]	Size (nm)	Polydispersity index	ζ-potential (mV)
FL	DSPC/Chol/ **1** = 56/39/1	-	134	0.05	-10.5
		+	136	0.19	-3.7
BL	DSPC/Chol = 56/39	-	106	0.04	-25.6
		+	98	0.11	-8.0

[a] In the absence (-) or presence (+) of IgG (IgG/**1** mole ratio = 1). Chol: cholesterol.

4.3.2. IgG-induced aggregation of FL.

The binding of IgG to FL was examined. Here I used FL with two kinds of concentrations, 0.1 and 1.0 mM in total lipid concentrations (**Figure 4.3**). In the both concentrations, aggregation of FL was observed when the IgG/**1** mixing ratio exceeded 10^{-2}, while the size of liposome recovered to be original size above the mixing ratio of **1**. Such IgG concentration dependent size change was not observed in BL. The mixing ratio dependent aggregation of FL will be due to the crosslinking of the liposome by IgG. Fc-III peptide binds to each heavy chain, thus the crosslinking of liposome possibly takes place (**Figure 4.4**).

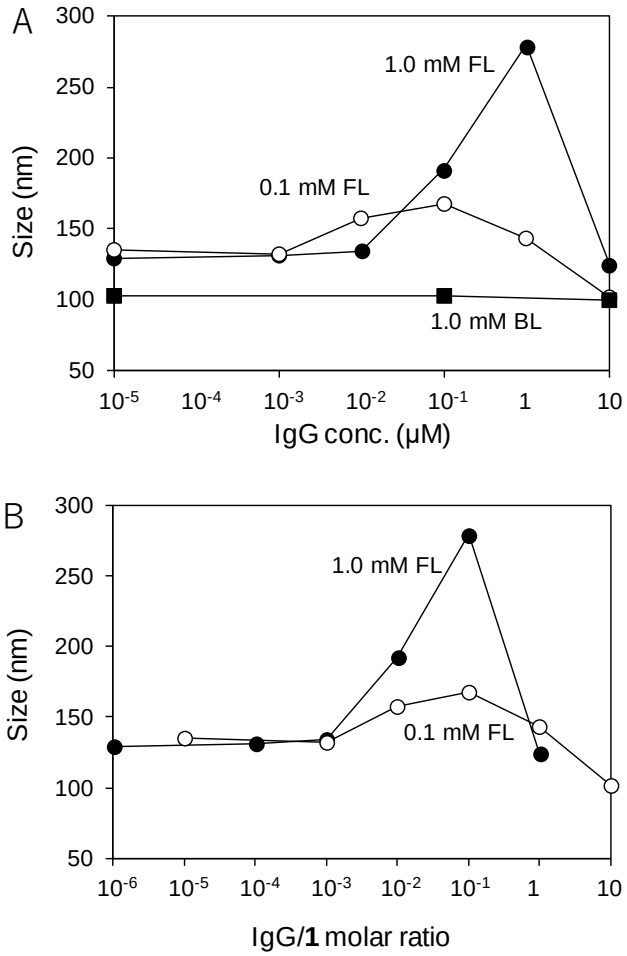

Figure 4.3. Change of liposome size in 10 mM HEPES containing different concentration of IgG (A). Repoltting of A by converting the x-axis mixing ratio of IgG/**1**. Total lipid concentration of FL and BLwas 0.1 or 1.0 mM. FL contains 1 mol% of **1**.

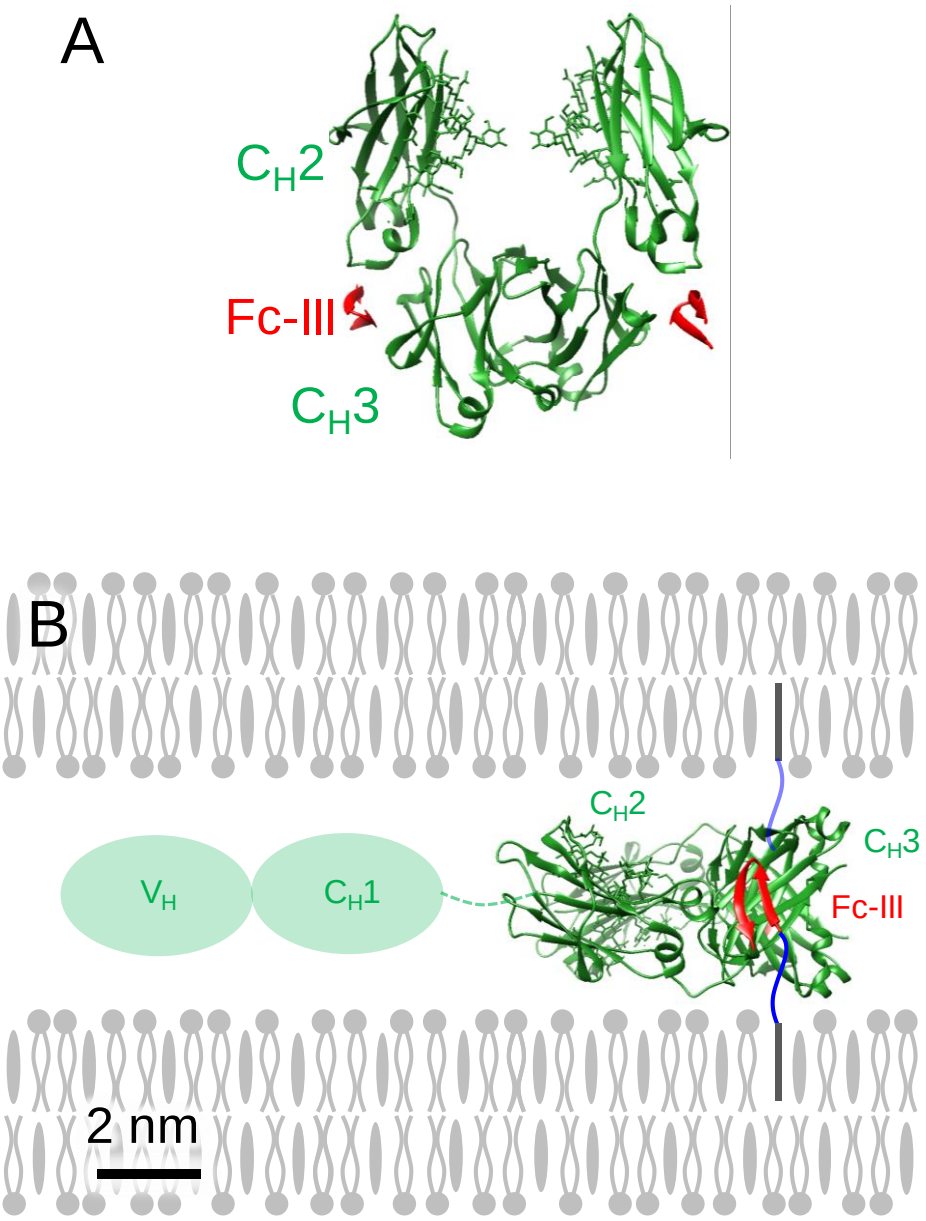

Figure 4.4. (A) Crystal structure of a complex between Fc-III peptide and Fc fragment (PDB ID: 1DN2). (B) Schematic drawing of crosslinking of Fc-III presenting liposomes via IgG. Each component of palmitate modified Fc-III peptide (**1**) are shown with different color: red, blue, and gray represent Fc-III peptide, hexaethyelneglycol linker, and palmitoyl, respectively.

4.3.3. Fluorescence Correlation Spectroscopy.

The binding of IgG to FL was further confirmed by using a point scan fluorescence correlation spectroscopy. IgG labeled with rhodamine was used here. **Figure 4.5** shows the fluorescence correlation curves of rhodamine-labelled IgG alone and its mixture with FL or BL. The correlation curves of IgG alone and IgG/BL mixture were almost overlapped, and diffusion time τ calculated from the curves were almost same (0.497 ms and 0.778 ms, respectively), indicating no interaction of IgG to BL. On the other hand, IgG/FL mixture (IgG/**1** mixing ratio = 0.01) showed much longer diffusion time (13.3 ms). The apparent hydrodynamic diameter (D_h) was calculated from the results of fitting of correlation curve based on Stokes-Einstein equation. D_h of IgG and IgG/BL were 20 and 31 nm, respectively. While, D_h of IgG/FL mixture was 528 nm, which is comparable to the size of the liposome. This is the clear evidence of binding of IgG to the FL surface.

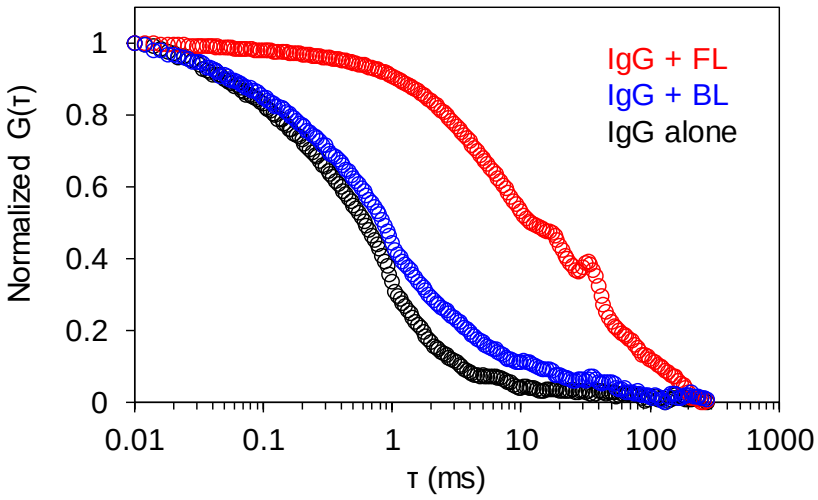

Figure 4.5. Normalized average FCS curves for rhodamine-labeled IgG (1 μM) with FL or BL (total lipid: 10 mM), or without liposomes in 10 mM HEPES buffer pH 7.4.

4.3.4. Interaction of IgG-coated FL to cells.

Finally, binding ability of IgG presented on FL surface to cellular membrane proteins was examined by using flow cytometry. FL was fluorescently labeled with DiO and anti-CD20 IgG was used to coat the FL surface. Two types of cells expressing CD20 for JY25 human B lymphoid cells and Fcγ receptors (FcγRs) (U937 monocyte) [15] were used here. FcγRs bind to C_H2 region of IgG to phagocytose objectives which are recognized by IgGs through valuable regions [16]. First, the expression of CD20 and FcγRs was confirmed (**Figure 4.6**). Expression of CD20 was confirmed by using anti-CD20 IgG (ofatumumab), while that of FcγRs was confirmed by mogamulizumab which is known to bind to have high affinity to one of the FcγRs [17,18]. As expected, the expression of CD20 was exclusively observed in JY25 cells, while that of FcγRs was exclusive in U937 cells.

As shown in **Figure 4.7A**, FL bound to CD20-positive JY25 cells, showing that anti-CD20 IgG on the FL surface maintains the binding ability to its complementary antigen. Small amount of FL and BL bound to FcγRs-positive U937 being independent of the IgG on liposome surface, indicating that the minor binding of FL to U937 cells are independent of FcγRs. I confirmed these observation in two types of cells by fluorescence microscopy (**Figure 4.7B**). The IgG-coated FL bound to CD20-positive JY25 cells, while the binding to FcγRs-positive cells, negative control U937 cells, was negligible. The negligible binding of IgG coated FL to FcγRs-positive cells will be crucial to avoid the recognition by macrophages during blood circulation.

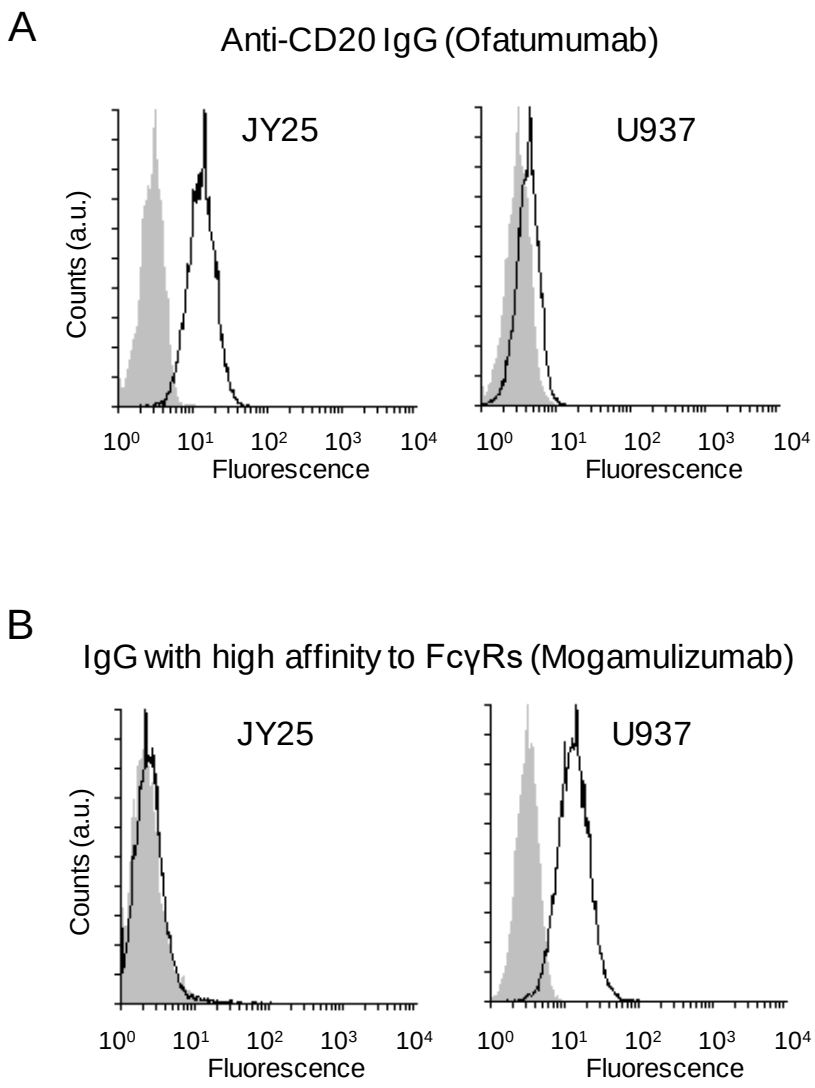

Figure 4.6. Expression of CD20 and FcγRs on cells was detected by flow cytometry analysis of the binding of rhodamine-labeled anti-CD 20 IgG (A) and fluorescein-labeled monoclonal IgG of mogamulizumab with high affinity to FcγRs (B), respectively. In A, ex. 470/40 nm; em. 585/40 nm. In B, ex. 470/40 nm; em. 535/50 nm. Grey-filled histograms represent the fluorescent background of cells.

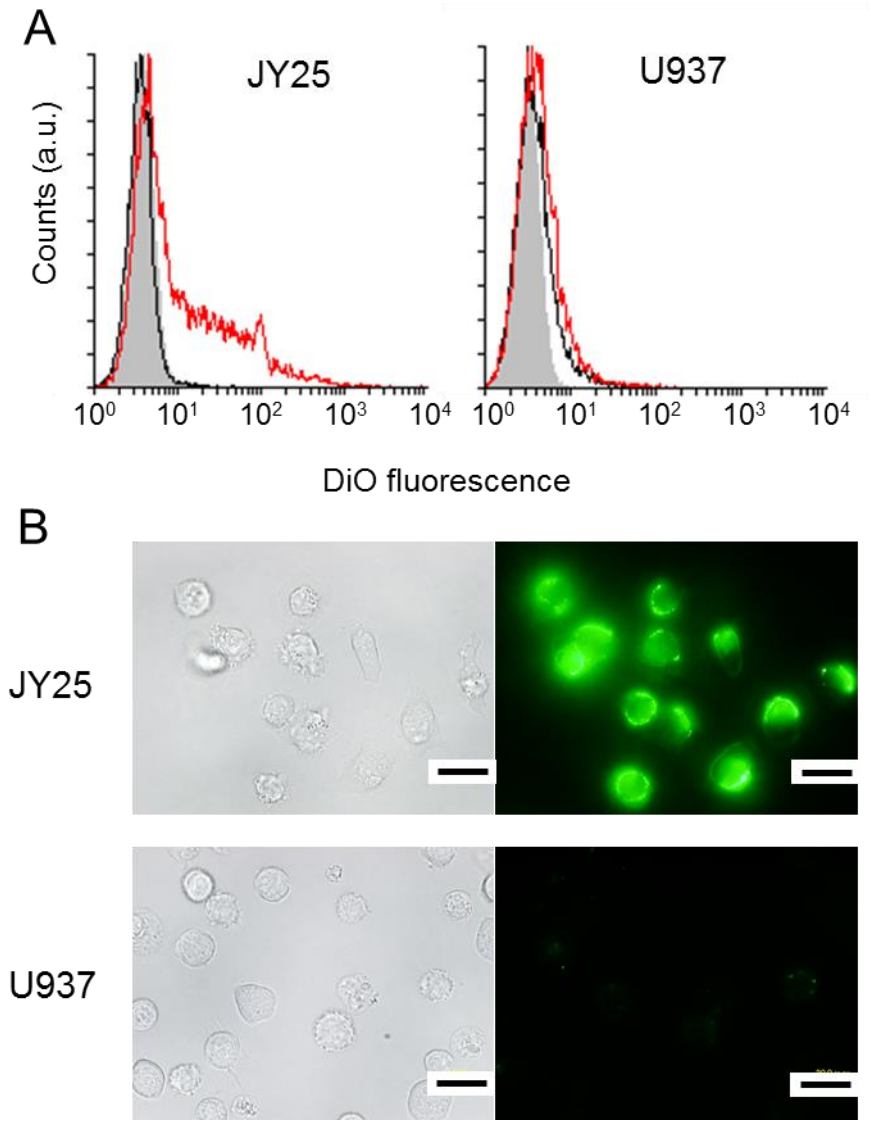

Figure 4.7. Binding of DiO-labeled liposomes to JY25 and U937 were observed using flow cytometry (ex. 488 nm; em. 525/50 nm) (A) and by flow cytometry (ex. 470/40 nm; em. 535/50 nm) (B). In A, red and black lines show FL and BL, respectively. Grey-filled histograms represent the fluorescent background of cells. In B, JY25 (upper panel) and U937 (lower panel). Left and right images are bright field and fluorescence images, respectively. Mole ratio of IgG/**1** was 0.5 in the both experiments. Scale bars: 20 μm.

4.4. Conclusions

I proposed here ligand-mediated coating of liposome with IgG through its constant region. The ligand-presenting liposome was coated with endogenous concentration of IgG. The resulting IgG-coated liposome was not recognized by macrophage via FcγRs. Thus, present strategy may enable *in situ* coating of liposome with endogenous IgG in blood to endow stealth characteristics to the liposomes for efficient drug delivery.

4.5. References

[1] Allen, T. M.; Hansen, C.; Martin, F.; Redemann, C.; Yau-Young, A. Liposomes containing synthetic lipid derivatives of poly(ethylene glycol) show prolonged circulation half-lives in vivo. *Biochim. Biophys. Acta* **1991**, *1066*, 29-36.

[2] Ishida, T.; Ichihara, M.; Wang, X.; Kiwada, H. Spleen plays an important role in the induction of accelerated blood clearance of PEGylated liposomes. *J. Controlled Release* **2006**, *115*, 243-250.

[3] Koide, H.; Asai, T.; Hatanaka, K.; Shimizu, K.; Yokoyama, M.; Ishida, T.; Kiwada, H.; Oku, N. Elucidation of accelerated blood clearance phenomenon caused by repeat injection of PEGylated nanocarriers. *Yakugaku Zasshi* **2009**, *129*, 1445-1451.

[4] Morell, A.; Terry, W. D.; Waldmann, T. A. Metabolic properties of IgG subclasses in man. *J. Clin. Invest.* **1970**, *49*, 673-680.

[5] Sidorin, E. V.; Solov'eva, T. F. IgG-bindin proteins of bacteria. *Biochemistry (Mosc.)* **2011**, *76*, 295-308.

[6] Akerström, B.; Brodin, T.; Reis, K.; Björck, L. Protein G: a powerful tool for binding and detection of monoclonal and polyclonal antibodies. *J. Immunol.* **1985**, *135*, 2589-2592.

[7] Moks, T.; Abrahmsén, L.; Nilsson B.; Hellman, U.; Sjöquist, J.; Uhlén, M. Staphylococcal protein A consists of five IgG-binding domains. *Eur. J. Biochem.* **1986**,*156*, 637-643.

[8] Nilsson, B.; Moks, T.; Jansson, B.; Abrahmsén, L.; Elmblad, A.; Holmgren, E.; Henrichson, C.; Jones, T. A.; Uhlén, M. A synthetic IgG-binding domain based on staphylococcal protein A. *Protein Eng.* **1987**, *1*, 107-113.

[9] Braisted, A. C.; Wells, J. A. Minimizing a binding domain from protein A. *Proc.*

Natl. Acad. Sci. USA **1996**, *93*, 5688-5692.

[10] Rorsgren, A.; Sjöquist, J. "Protein A" from S. aureus. I. Pseudo-immune reaction with human γ-globulin. *J. Immunol.* **1966**, *97*, 822-827.

[11] Björck, L.; Kronvall, G. Purification and some properties of streptococcal protein G, a novel IgG-binding reagent. *J. Immunol.* **1984**, *133*, 969-974.

[12] Delano, W. L.; Ultsch, M. H.; de Vos, A. M.; Wells, J. A. Convergent solutions to binding at a protein-protein interface. *Science*, **2000**, 287, 1279-1283.

[13] Boonyarattanakalin,S.; Martin, S. E.; Sun, Q.; Peterson, B. R. A synthetic Mimic of Human Fc Receptors: Defined Chemical Modification of Cell Surfaces Enables Efficient Endocytic Uptake of Human Immunoglobulin-G, *J. Am. Chem. Soc.* **2006**, 128, 11463-11470.

[14] Tam, J. P.; Wu, C. R.; Liu, W.; Zhang, J. W. Disulfide bond formation in peptides by dimethyl sulfoxide. Scope and applications. *J. Am. Chem. Soc.* **1991**, *113*, 6657-6662.

[15] Kecse-Nagy, C.; Szittner, Z.; Papp, K.; Hegyi, Z.; Rovero, P.; Migliorini, P. Lóránd, V.; Homolya, L.; Prechl, J. Characterization of NF-κB reporter U937 cells and their application for the detection of inflammatory immune-complexes. *PLoS One.* **2016**, *11*, e0156328.

[16] Jefferis, R.; Lund, J. Interaction sites on human IgG-Fc for FcgammaR: current models. *Immunol. Lett.* **2002**, *82*, 57-65.

[17] Ishii, T.; Ishida, T.; Utsunomiya, A.; Inagaki, A.; Yano, H.; Komatsu, H.; Iida, S.; Imada, K.; Uchiyama, T.; Akinaga, S.; Shitara, K.; Ueda, R. Defucosylated humanized anti-CCR4 monoclonal antibody KW-0764 as a novel immunotherapeutic agent for adult T-cell leukemia/lymphoma. *Clin. Cancer Res.* **2010**, *16*, 1520-1531.

[18] Ishida, T.; Ueda, R. CCR4 as a novel molecular target for immunotherapy of

cancer. *Cancer Sci.* **2006**, *97*, 1139-1146.

CHAPTER 5

General Conclusions

Surface modification of liposome enables the potential therapeutic application by enhancing the stability to prolong the blood residence time and specificity to target cell to deliver drugs. Human serum albumin and IgG are known to have long blood half-life and the biological roles such as carrier of endogenous small molecules for serum albumin, and immune activity for IgG, and which have been applied to drug carriers. There are several reports of serum albumin, which showed to improve the colloidal stability and prevent opsonization. The proteins have been covalently and non-covalently immobilized on the surface. However, despite the abundance of endogenous serum albumin and IgG in blood, liposomes binding to them in blood are quite rare. Furthermore, specific interaction between ligand and the protein has been expected to modulate the denaturation of the proteins. Here, I proposed novel liposome modification methods using ligands for such proteins.

In Chapter 2 and 3, serum albumin-modified liposomes were exploited. Numerous ligand binding to serum albumin have been investigated. Among them, in Chapter 2, I selected bilirubin, which has two carboxyl groups. One of the carboxyl groups was used to modify on lipid and the other one was expected to work to prevent burying in liposome hydrophobic membrane. Because the liposome was difficult to be dissolved in aqueous solution due to high hydrophobic ligand, alkaline buffer was used to hydrate the liposome. The obtained liposome was reversibly coated with serum albumin. In Chapter 3, I selected alkyl chains with different length and with or without a negative charge on the terminus. A ligand mediated coated liposome enabled

hydrophobic ligand to be presented on liposome surface without aggregation, and succeeded to be coated with serum albumin. This liposome was as inert as PEGylated liposomes to phagocytotic uptake by macrophages. Compared with covalent modification, non-covalent coating reported here is advantageous because the coating can be applied at the time of use by mixing with fresh serum albumin.

In Chapter 4, I proposed Fc-III peptide mediated coating of liposome with IgG. Fc-III peptide was modified with palmitic acid on N-terminus to bind on the liposomal membrane. The liposome presenting palmitoylated Fc-III was successfully coated with IgG, which was confirmed by fluorescence correlation spectrometry and IgG-mediated binding to the antigen-presenting cell. The uptake of the liposome by monocytic cells was low level, indicating that IgG-coated liposome is not recognized by FcγRs of macrophage. Thus the IgG-coated liposome will not be captured by macrophage, leading to the extended blood circulation.

In this thesis, ligand-mediated surface coating was expected to avoid denaturation of coating protein. As I mentioned, the surface coating by physical adsorption causes denaturation of the serum albumin in some cases [1,2]. In the case of physical coating of HSA on liposome, we found that the liposome is aggregated (in section 3.3.4). This aggregation will be induced by the adsorption of HSA on the liposome. In contrast, the liposomes coated with HSA via ligand dispersed stably. The coated HSA seems to maintain native conformation due to the specific interaction between HSA and ligand.

Low-fouling or nonfouling polymer coating has been achieved by hydrophilic polymers (e.g. PEG, poly(2-methyl-2-oxazoline)) [3,4], zwitterionic polymers (e.g. poly(2-methacryloyloxyethyl phosphorylcholine), poly(carboxybetaine acrylamide))

[5,6], and polymers with microphase-separated structure (e.g. poly(2-hydroxyethyl methacrylate-*block*-polystyrene, poly(methyl methacrylate) grafted with poly(hydroxyethyl methacrylate)) [7,8]. These polymer coatings can protect the surface from protein adsorption, coagulation, and platelet aggregation. This is because they have hydrophilic nature, electrically neutrality, and hydrogen-bond acceptors/donors, and chain flexibility [9]. The hydrated water on the polymer is classified to three types in the order from the surface; non-freezing water, intermediate water, and free water [10]. Intermediate water, which is proposed by Tanaka *et al.*, is weakly bound to the surface or non-freezing water, and prevents the binding of proteins and blood cells to the surface [10]. Furthermore, biopolymers including serum albumin and hyaluronic acid, which have been used to coat the surface of materials to provide bio/blood compatibility, are also reported to show cold-crystallization of intermediate water [11,12].

To develop the anti-fouling liposome, synthetic and natural polymers with intermediate water will be useful. The proteins-coated liposomes proposed in this thesis are prepared by using synthetic polymer (PEG) and natural polymer (HSA), both of which have intermediate water.

Perspectives

In this thesis, I achieved the development of ligand-mediated coating of liposome with serum albumin and IgG. I elucidated the importance of the length of alkyl chain and terminal charge for the albumin binding. As for the IgG coating, Fc-III peptide works to present IgG on liposome surface. These findings will lead to exploiting more practical ligand-mediated liposomes. Conventional covalent modification of liposome with proteins conducted by using reactive residues such as lysine and cysteine [13]. Such process takes time and cannot control the modification residue of proteins. However, ligand-mediated coating can coat the liposome surface by mixing with fresh serum albumin and IgG. The ligand-mediated coating will be able to protect HSA and IgG from denaturation, resulting in developing long-acting and highly specific and effective protein-modified liposomes, and additionally may be convenient process for production. The ligand-mediated coating will bring new function to liposome, which is not expected from covalent-coating. Indeed, ligand-mediated coated liposome with serum albumin showed as inert as PEG-modified liposome to macrophage uptake, and the result was different from that of covalent coating [14]. HSA-coated liposome may enhance accumulation in tumor through albumin specific receptor expressed in endothelial cells and tumor cells. On the other hand, IgG-coated liposome via Fc-III peptide showed binding to the cells expressing the receptor to the IgG's variable region, while the liposome was not recognized by monocytes expressing the receptor to IgG's Fc region. IgG-coated liposomes may have stealth characteristics and show long blood circulation. Recently, specific ligands for proteins have intensively been studied. These ligands also will be useful for the ligand mediated coating strategy.

This ligand-mediated coating of liposome with protein may provide an extension

of current liposomes technology because most of conventional protein modified carrier was prepared by covalent coating. I believe that this strategy is useful for developing the drug carriers that not only exhibit effective functions in patient body but also be produced in convenient process and show constant quality.

References

[1] Vermonden, T.; Giacomelli, C. E.; Norde, W. Reversibility of structural rearrangements in bovine serum albumin during homomolecular exchange from AgI particles. *Langmuir* **2001**, *17*, 3734-3740.

[2] Norde, W.; Giacomelli, C. E. BSA structural changes during homomolecular exchange between the adsorbed and the dissolved states. *J. Biotechnol.* **2000**, *79*, 259-268.

[3] Kingshott, P.; Wei, J.; Bagge-Ravn, D.; Gadegaard, N.; Gram, L. Covalent attachment of poly(ethylene glycol) to surfaces, criticcacl for reducing bacterial adhesion. *Langmuir* **2003**, *19*, 6912-6921.

[4] Konradi, R.; Pidhatika, B.; Muhlebach, A.; Textort, M. Poly-2-methyl-2-oxazoline: A peptide-like polymer for protein-repellent surfaces. *Langmuir* **2008**, *24*, 613-616.

[5] Ishihara, K.; Hasegawa, T.; Watanabe, J.; Iwasaki, Y. Protein adsorption-resistant hollow fibers for blood purification. *Artif. Organs* **2002**, *26*, 1014-1019.

[6] Yang, W.; Chen, S.; Cheng, G. Vaisocherová, H.; Xue, H.; Li, W.; Zhang, J.; Jiang, S. Film thickness dependence of protein adsorption from blood serum and plasma onto poly(sulfobetaine)-grafted surfaces. *Langmuir* **2008**, *24*, 9211-9214.

[7] Okano, T.; Nishiyama, S. Shinohara, I.; Akaike, T.; Sakurai, Y.; Kataoka, K.; Tsuruta, T. Effect of hydrophilic and hydrophobic microdomains on mode of interaction between block polymer and blood platelets. *J. Biomed. Mater. Res.* **1981**, *15*, 393-402.

[8] Nakashima, T.; Takakura, K.; Komoto, Y. Thromboresistance of graft-type copolymers with hydrophilic-hydrophobic microphase-separated structure. *J. Biomed. Mater. Res.* **1977**, *11*, 787-798.

[9] Chen, S.; Li, L.; Zhao, C.; Zheng, J. Surface hydration: Principles and applications

toward low-fouling/nonfouling biomaterials. *Polymer* **2010**, *51*, 5283-5293.

[10] Tanaka, M.; Hayashi, T.; Morita, S. The roles of water molecules at the biointerface of medical polymers. *Polym. J.*, **2013**, *45*, 701-710.

[11] Panagopoulou, A.; Kyritsis, A.; Sabater i Serra, R.; Gómez Ribelles, J. L.; Shinyashiki, N., Pissis, P. Glass transition and dynamics in BSA–water mixtures over wide ranges of composition studied by thermal and dielectric techniques. *Biochim. Biophys. Acta* **2011**, *1814*, 1984-1996.

[12] Hatakeyama, H.; Hatakeyama, T. Interaction between water and hydrophilic polymers. *Thermochim. Acta* **1998**, *308*, 3-22.

[13] Nobs, L.; Buchegger, F.; Gurny, R.; Allémann, E. Current methods for attaching targeting ligands to liposome and nanoparticles. *J. Pham. Sci.* **2004**, *93*, 1980-1992.

[14] Vuarchey, C.; Kumar, S.; Schwendener, R. Albumin coated liposomes: a novel platform for macrophage specific drug delivery. *Nanotechnol. Devel.* **2011**, *1*, e2.

Accomplishments

Publications

1. **Sato, H.**; Nakhaei, E.; Kawano, T.; Murata, M.; Kishimura, A.; Mori, T.; Katayama, Y. Ligand-Mediated Coating of Liposomes with Human Serum Albumin. *Langmuir* in press
2. **Sato, H.**; Nakamura, Y.; Nakhaei, E.; Funamoto, D.; Kim, C. W.; Yamamoto, T.; Kishimura, A.; Mori, T.; Katayama, Y. A liposome reversibly coated with serum albumin. *Chem. Lett.* **2014**, *43*, 1481-1483.
3. Nakamura, Y.; **Sato, H.**; Nobori, T.; Matsumoto, H.; Toyama, S.; Shuno, T. Kishimura, A.; Mori, T.; Katayama, Y. Modification of ligands for serum albumin on polyethyleneimine to stabilize polyplexes in gene delivery. *J. Biomater. Sci. Polym. Ed.* **2017**, *28*, 1382-1393.
4. Nakhaei, E.; Kim, C. W.; Funamoto, D.; **Sato, H.**; Nakamura, Y.; Kishimura, A.; Mori, T.; Katayama, Y. Design of a ligand for cancer imaging with long blood circulation and an enhanced accumulation ability in tumors. *Med. Chem. Comm*. **2017**, *8*, 1190-1195.
5. Tahara, Y.; Yoshikawa, T.; **Sato, H.**; Mori, Y.; Hosain, Z.; Kishimura, A.; Mori, T.; Katayama, Y. Encapsulation of a nitric oxide-donor into a liposome to boost the enhanced permeation and retention (EPR) effect. *Med. Chem. Comm*. **2017**, *8*, 415-421.
6. Li, K.; **Sato, H.**; Kim, C. W.; Nakamura, Y.; Zhao, G. X.; Funamoto, D.; Nobori, T.; Kishimura, A.; Mori, T.; Katayama, Y. Tumor accumulation of protein kinase-responsive gene carrier/DNA polyplex stabilized by alkanethiol for intravenous injection. *J. Biomater. Sci., Polym. Ed*. **2015**, *26*, 657-668.
7. Funamoto, D.; Asai, D.; Sato, K.; Yamaguchi, Y.; Kim, C. W.; **Sato, H.**; Nakhaei,

E.; Matsumoto, S.; Yoshikawa, T.; Sasaki, K.; Yamamoto, T.; Kishimura, A.; Mori, T.; Katayama, Y. Antibody Internalization into Living Cell via Crosslinker-mediated Endocytosis. *Chem. Lett*. **2015**, *44*, 468-470.

International oral presentation

1. “Liposomal carrier coated with serum albumin via long alkyl chain as a ligand”, Biomaterials International 2017, Fukuoka, Japan, August 2017

International poster presentations

1. “A liposome coated with serum albumin via long alkyl chain as a ligand”, ICONAN 2017, Barcelona, Spain, September 2017
2. “Development of a Long-circulating Liposomal Carrier Coated with Serum Albumin via Ligand”, ICONAN 2016, Paris, France, September 2016
3. “Improvement of Blood Circulation Time of Liposome by Coating with Serum Albumin via Ligand”, ChinaNanomedicine 2016, Wuhan, China, October 2016, **Poster Award**
4. “Reversible coating of liposome with serum albumin for improved blood circulation”, Pacifichem 2015, Honolulu, Hawaii, December 2015
5. “Improvement of Circulation Time of Liposomal Carrier by Reversibly Covering with Serum Albumin”, The 15th IUMRS-International Conference in Asia, Fukuoka, August 2014

Domestic oral presentation

1. 「血清アルブミンの可逆的な被覆によるリポソーム性キャリアの血中滞留性の向上」、第 63 回高分子学会年次大会、名古屋、2014 年 5 月

Domestic poster presentations

1. 「バクテリアに学ぶリポソームの長期血中循環の戦略:アルブミンによる可逆的被覆」、第 32 回日本 DDS 学会学術集会、静岡、2016 年 6 月
2. 「血清アルブミンの可逆的被覆による高血中滞留性リポソームの開発」、第 4 回 CSJ 化学フェスタ 2014、東京、2014 年 10 月
3. 「可逆的なアルブミン被覆を利用した長期血中循環型リポソームの開発」、バイオマテリアル学会九州ブロック講演会、福岡、2014 年 9 月
4. 「アルブミンの被覆によるキャリアの血中滞留性の向上」、平成 25 年度九州地区高分子若手研究会・冬の講演会、福岡、2013 年 12 月

Acknowledgement

Firstly, I wish to express my sincere gratitude to my supervisor, Prof. Yoshiki Katayama for providing great research environment to study this thesis in his laboratory and his considerable instruction and encouragement.

I would like to express my deepest appreciation to Prof. Takeshi Mori for his great instruction, suggestion, and all his time in helping and encouraging me to complete this thesis. Moreover, I also express my grateful gratitude to Prof. Akihiro Kishimura for invaluable advice and encouragement. I want to thank Prof. Tatsuhiro Yamamoto for kind instruction and advice in experiment.

I am grateful to my doctoral thesis committee members, Prof. Masamichi Kamihira, and Prof. Masaru Tanaka for their fruitful discussion and invaluable advices.

I thank Prof. Masahiro for the use of flow cytometry, and Prof. Masaharu Murata and Dr. Takahito Kawano for the use of fluorescence correlation spectroscopy. I also thank the Japan Society for the Promotion of Science (JSPS) KAKENHI Grand-in-Aid for Research Fellows (JP16J04193) and gratitude to the Program for Leading Graduate Schools, Graduate education and research training program in DECISION SCIENCE for a sustainable society, for their financial supports.

I also express my special thanks to my D-RECS and s-DDS group members, Dr. Chan Woo Kim (Catholic University of Korea), Dr. Daiki Funamoto (Kyushu University), Dr. Eun Kyung Lee, Dr. Md. Zahangir Hosain, Mr. Kai Li, Ms. Elnaz Nakhaei, Mr. Takanobu Nobori, Mr. Yu Tahara, Ms. Ayako Yanagida, Mr. Kohichi Sasaki, Mr. Takuma Yoshikawa, Mr. Haitao Feng, Ms. Yukina Mori, Mr. Yoshiki Miyashita, Mr. Yusuke Nagao, Ms. Minori Harada, Mr. Toru Kosaka, and Mr. Phan Quoc Khanh, for their suggestion, assistance of the experiments and encouragement. I would like to especially thank Dr. Yuta Nakamura and Dr. Hengmin Tang for their

great advice, help and encouragement during my laboratory life. I also thank the all students and Ms. Mari Miyazaki of Katayama laboratory for their help in experiments, and practical and emotional supports.

I would like to acknowledge all persons who relate to this thesis.

Finally, I appreciate my family, Mr. Kiminori Sato, Ms. Fujiko Sato, and Aya Sato for constant support and encouragement through all these years of study.

February 2018

Hikari Sato